though their unique functions have yet to be characterized (35). These TTP-related proteins are rapidly expressed in response to 12-*O*-tetradecanoylphorbol-13-acetate and other diverse stimuli in various types of eukaryotic cells (23,36). The expression of these proteins differs depending on the circumstances, hence they may have their own roles in controlling mRNA turnover under different circumstances (37). Among these proteins, TTP is induced by TNFα, suggesting that TTP may function as a feedback regulator of TNFα gene expression (31,38). Notably, a TIS11B homolog expressed rapidly in response to butyrate has also been discovered in human cells and characterized as butyrate response factor 1 (BRF1) (39).

Consistently, butyrate rapidly induced the expression of TIS11B in RAW264.7 cells (Figure 4A). In addition, the induction of TNFα mRNA by LPS stimulation was strongly inhibited when TIS11B was overexpressed in these cells (Figure 4B). Stoecklin et al identified BRF1 as a regulator of ARE-dependent mRNA decay, and also showed that BRF1 can bind directly to ARE and promote the degradation of ARE-containing mRNA (40). Thus, we postulated a model whereby butyrate induced the expression of TIS11B/BRF1, followed by the binding of this ARE-binding protein to the ARE, thus facilitating TNFα mRNA degradation. Our cDNA microarray (GeneNavigator cDNA Array System; Toyobo) revealed that butyrate suppressed expression of mRNA containing AREs in their 3′-UTRs (e.g., mRNA for IL-1β, IL-15, and granulocyte–macrophage colony-stimulating factor) (data not shown). This result further supported the relevance of our hypothesis.

TIS11B has a unique character that facilitates TNFα mRNA degradation; therefore, analyzing the regulation of this molecule would provide a novel approach to the control of TNFα production. TNFα expression is activated mainly by the transcription factor NF-κB and by the MAP kinase (MAPK) pathways (the ERK, JNK, and p38 MAPK pathways). Recent studies have shown that the p38 MAPK pathway in particular plays an important role in posttranscriptional regulation that leads to mRNA stabilization (41). The p38 MAPK pathway also strongly induces and activates TTP, which down-regulates TNFα (42–45). Those studies suggested that the p38 MAPK pathway may play a crucial role in regulating the expression of TNFα (involving a TTP-dependent mechanism); however, the precise mechanism is not completely understood, and less is known about the relationship between TIS11B and the p38 MAPK pathway. Since butyrate induced TIS11B expression and has been shown to affect the p38 MAPK pathway (46), it may be that butyrate influences TIS11B expression through the p38 MAPK pathway. Analysis of the relationship between TIS11B and the p38 MAPK pathway would be important for understanding the effect of butyrate.

The effects of butyrate on TNFα gene expression, other than those involving TIS11B- and ARE-dependent mechanisms, also need to be addressed. In previous studies, it was shown that butyrate can inhibit the binding of NF-κB to DNA (12,15,47). In contrast, in the reporter gene assays, butyrate enhanced the transcriptional activity driven by NF-κB sites and the TNFα promoter in a dose-dependent manner (Figures 3A and B). This phenomenon may be explained in part by the HDA-inhibitory effects of butyrate. Butyrate strongly inhibits HDA activity in cells, and it can cause hyperacetylation of nucleotides and thereby nonspecifically enhance transcriptional activity (18,48,49). As in the case of genomic DNA, transfected plasmid DNA has been shown to be assembled with histones to form a "minichromosome" that is sensitive to histone hyperacetylation (50). Thus, butyrate can function as a nonspecific transcriptional enhancer for transfected plasmid DNA; hence, cotransfection with an internal control was not informative in the current experiments.

Analysis of the regulation of TNFα by butyrate provides information for a novel approach to the treatment of patients with RA. Further investigation of the regulation of TIS11B expression, including study of its gene promoter, promises to pave the way for therapeutic approaches that address ARE-dependent cytokine gene regulation.

ACKNOWLEDGMENTS

We thank Ms Akiko Hirano and Ms Miki Aoto for technical assistance.

REFERENCES

1. Feldmann M, Brennan FM, Maini RN. Rheumatoid arthritis. Cell 1996;85:307–10.
2. Daniel CL, Moreland LW. Infliximab: additional safety data from an open label study. J Rheumatol 2002;29:647–9.
3. MacNaul KL, Chartrain N, Lark M, Tocci MJ, Hutchinson NI. Discoordinate expression of stromelysin, collagenase, and tissue inhibitor of metalloproteinases-1 in rheumatoid human synovial fibroblasts: synergistic effects of interleukin-1 and tumor necrosis factor-α on stromelysin expression. J Biol Chem 1990;265:17238–45.
4. Chin JE, Winterrowd GE, Krzesicki RF, Sanders ME. Role of cytokines in inflammatory synovitis: the coordinate regulation of

intercellular adhesion molecule 1 and HLA class I and class II antigens in rheumatoid synovial fibroblasts. Arthritis Rheum 1990;33:1776–86.
5. Feldmann M, Brennan FM, Chantry D, Haworth C, Turner M, Abney E, et al. Cytokine production in the rheumatoid joint: implications for treatment. Ann Rheum Dis 1990;49:480–6.
6. Chu CQ, Field M, Feldmann M, Maini RN. Localization of tumor necrosis factor α in synovial tissues and at the cartilage–pannus junction in patients with rheumatoid arthritis. Arthritis Rheum 1991;34:1125–32.
7. Tak PP, Bresnihan B. The pathogenesis and prevention of joint damage in rheumatoid arthritis: advances from synovial biopsy and tissue analysis [review]. Arthritis Rheum 2000;43:2619–33.
8. Takayanagi H, Oda H, Yamamoto S, Kawaguchi H, Tanaka S, Nishikawa T, et al. A new mechanism of bone destruction in rheumatoid arthritis: synovial fibroblasts induce osteoclastogenesis. Biochem Biophys Res Commun 1997;240:279–86.
9. Zhang G, Ghosh S. Molecular mechanisms of NF-κB activation induced by bacterial lipopolysaccharide through Toll-like receptors. J Endotoxin Res 2000;6:453–7.
10. Choe JY, Crain B, Wu SR, Corr M. Interleukin 1 receptor dependence of serum transferred arthritis can be circumvented by toll-like receptor 4 signaling. J Exp Med 2003;197:537–42.
11. Bamba T, Kanauchi O, Andoh A, Fujiyama Y. A new prebiotic from germinated barley for nutraceutical treatment of ulcerative colitis. J Gastroenterol Hepatol 2002;17:818–24.
12. Inan MS, Rasoulpour RJ, Yin L, Hubbard AK, Rosenberg DW, Giardina C. The luminal short-chain fatty acid butyrate modulates NF-κB activity in a human colonic epithelial cell line. Gastroenterology 2000;118:724–34.
13. Weaver GA, Krause JA, Miller TL, Wolin MJ. Short chain fatty acid distributions of enema samples from a sigmoidoscopy population: an association of high acetate and low butyrate ratios with adenomatous polyps and colon cancer. Gut 1988;29:1539–43.
14. Kashtan H, Stern HS, Jenkins DJ, Jenkins AL, Thompson LU, Hay K, et al. Colonic fermentation and markers of colorectal-cancer risk. Am J Clin Nutr 1992;55:723–8.
15. Segain JP, Raingeard de la Bletiere D, Bourreille A, Leray V, Gervois N, Rosales C, et al. Butyrate inhibits inflammatory responses through NFκB inhibition: implications for Crohn's disease. Gut 2000;47:397–403.
16. Ahmad MS, Krishnan S, Ramakrishna BS, Mathan M, Pulimood AB, Murthy SN. Butyrate and glucose metabolism by colonocytes in experimental colitis in mice. Gut 2000;46:493–9.
17. Pazin MJ, Kadonaga JT. What's up and down with histone deacetylation and transcription? Cell 1997;89:325–8.
18. Espinos E, Le V, Thai A, Pomies C, Weber MJ. Cooperation between phosphorylation and acetylation processes in transcriptional control. Mol Cell Biol 1999;19:3474–84.
19. Atsumi T, Nishihira J, Makita Z, Koike T. Enhancement of oxidised low-density lipoprotein uptake by macrophages in response to macrophage migration inhibitory factor. Cytokine 2000; 12:1553–6.
20. Heid CA, Stevens J, Livak KJ, Williams PM. Real time quantitative PCR. Genome Res 1996;6:986–94.
21. Chen J, Amasaki Y, Kamogawa Y, Nagoya M, Arai N, Arai K, et al. Role of NFATx (NFAT4/NFATc3) in expression of immunoregulatory genes in murine peripheral CD4+ T cells. J Immunol 2003;170:3109–17.
22. Semon D, Kawashima E, Jongeneel CV, Shakhov AN, Nedospasov SA. Nucleotide sequence of the murine TNF locus, including the TNF-α (tumor necrosis factor) and TNF-β (lymphotoxin) genes. Nucleic Acids Res 1987;15:9083–4.
23. Ino T, Yasui H, Hirano M, Kurosawa Y. Identification of a member of the TIS11 early response gene family at the insertion point of a DNA fragment containing a gene for the T-cell receptor β chain in an acute T-cell leukemia. Oncogene 1995;11:2705–10.
24. Amasaki Y, Adachi S, Ishida Y, Iwata M, Arai N, Arai K, et al. A constitutively nuclear form of NFATx shows efficient transactivation activity and induces differentiation of CD4(+)CD8(+) T cells. J Biol Chem 2002;277:25640–8.
25. Van den Berg WB, van Lent PL. The role of macrophages in chronic arthritis. Immunobiology 1996;195:614–23.
26. McCarthy JE, Kollmus H. Cytoplasmic mRNA-protein interactions in eukaryotic gene expression. Trends Biochem Sci 1995;20: 191–7.
27. Xu N, Chen CY, Shyu AB. Modulation of the fate of cytoplasmic mRNA by AU-rich elements: key sequence features controlling mRNA deadenylation and decay. Mol Cell Biol 1997;17:4611–21.
28. Peng SS, Chen CY, Shyu AB. Functional characterization of a non-AUUUA AU-rich element from the c-jun proto-oncogene mRNA: evidence for a novel class of AU-rich elements. Mol Cell Biol 1996;16:1490–9.
29. Bakheet T, Frevel M, Williams BR, Greer W, Khabar KS. ARED: human AU-rich element-containing mRNA database reveals an unexpectedly diverse functional repertoire of encoded proteins. Nucleic Acids Res 2001;29:246–54.
30. Bakheet T, Williams BR, Khabar KS. ARED 2.0: an update of AU-rich element mRNA database. Nucleic Acids Res 2003;31: 421–3.
31. Carballo E, Lai WS, Blackshear PJ. Feedback inhibition of macrophage tumor necrosis factor-α production by tristetraprolin. Science 1998;281:1001–5.
32. Taylor GA, Carballo E, Lee DM, Lai WS, Thompson MJ, Patel DD, et al. A pathogenetic role for TNFα in the syndrome of cachexia, arthritis, and autoimmunity resulting from tristetraprolin (TTP) deficiency. Immunity 1996;4:445–54.
33. Carballo E, Gilkeson GS, Blackshear PJ. Bone marrow transplantation reproduces the tristetraprolin-deficiency syndrome in recombination activating gene-2 (−/−) mice: evidence that monocyte/macrophage progenitors may be responsible for TNFα overproduction. J Clin Invest 1997;100:986–95.
34. Phillips K, Kedersha N, Shen L, Blackshear PJ, Anderson P. Arthritis suppressor genes TIA-1 and TTP dampen the expression of tumor necrosis factor α, cyclooxygenase 2, and inflammatory arthritis. Proc Natl Acad Sci U S A 2004;101:2011–6.
35. Johnson BA, Geha M, Blackwell TK. Similar but distinct effects of the tristetraprolin/TIS11 immediate-early proteins on cell survival. Oncogene 2000;19:1657–64.
36. Varnum BC, Ma QF, Chi TH, Fletcher B, Herschman HR. The TIS11 primary response gene is a member of a gene family that encodes proteins with a highly conserved sequence containing an unusual Cys-His repeat. Mol Cell Biol 1991;11:1754–8.
37. Blackshear PJ. Tristetraprolin and other CCCH tandem zinc-finger proteins in the regulation of mRNA turnover. Biochem Soc Trans 2002;30:945–52.
38. Lai WS, Carballo E, Strum JR, Kennington EA, Phillips RS, Blackshear PJ. Evidence that tristetraprolin binds to AU-rich elements and promotes the deadenylation and destabilization of tumor necrosis factor α mRNA. Mol Cell Biol 1999;19: 4311–23.
39. Maclean KN, McKay IA, Bustin SA. Differential effects of sodium butyrate on the transcription of the human TIS11 family of early-response genes in colorectal cancer cells. Br J Biomed Sci 1998;55:184–91.
40. Stoecklin G, Colombi M, Raineri I, Leuenberger S, Mallaun M, Schmidlin M, et al. Functional cloning of BRF1, a regulator of ARE-dependent mRNA turnover. EMBO J 2002;21:4709–18.
41. Wang SW, Pawlowski J, Wathen ST, Kinney SD, Lichenstein HS, Manthey CL. Cytokine mRNA decay is accelerated by an inhibitor of p38-mitogen-activated protein kinase. Inflamm Res 1999;48:533–8.
42. Dean JL, Sully G, Clark AR, Saklatvala J. The involvement of AU-rich element-binding proteins in p38 mitogen-activated pro-

tein kinase pathway-mediated mRNA stabilisation. Cell Signal 2004;16:1113–21.
43. Mahtani KR, Brook M, Dean JL, Sully G, Saklatvala J, Clark AR. Mitogen-activated protein kinase p38 controls the expression and posttranslational modification of tristetraprolin, a regulator of tumor necrosis factor α mRNA stability. Mol Cell Biol 2001;21: 6461–9.
44. Tchen CR, Brook M, Saklatvala J, Clark AR. The stability of tristetraprolin mRNA is regulated by mitogen-activated protein kinase p38 and by tristetraprolin itself. J Biol Chem 2004;279: 32393–400.
45. Brooks SA, Connolly JE, Rigby WF. The role of mRNA turnover in the regulation of tristetraprolin expression: evidence for an extracellular signal-regulated kinase-specific, AU-rich element-dependent, autoregulatory pathway. J Immunol 2004;172:7263–71.
46. Daniel C, Schroder O, Zahn N, Gaschott T, Stein J. p38 MAPK signaling pathway is involved in butyrate-induced vitamin D receptor expression. Biochem Biophys Res Commun 2004;324: 1220–6.
47. Venkatraman A, Ramakrishna BS, Shaji RV, Kumar NS, Pulimood A, Patra S. Amelioration of dextran sulfate colitis by butyrate: role of heat shock protein 70 and NF-κB. Am J Physiol Gastrointest Liver Physiol 2003;285:G177–84.
48. Boffa LC, Vidali G, Mann RS, Allfrey VG. Suppression of histone deacetylation in vivo and in vitro by sodium butyrate: reversible effects of Na-butyrate on histone acetylation. J Biol Chem 1978; 253:3364–6.
49. Vidali G, Boffa LC, Mann RS, Allfrey VG. Reversible effects of Na-butyrate on histone acetylation. Biochem Biophys Res Commun 1978;82:223–7.
50. Reeves R, Gorman CM, Howard B. Minichromosome assembly of non-integrated plasmid DNA transfected into mammalian cells. Nucleic Acids Res 1985;13:3599–615.

Excessive exposure to anionic surfaces maintains autoantibody response to β_2-glycoprotein I in patients with antiphospholipid syndrome

Yukie Yamaguchi,[1,2] Noriyuki Seta,[1] Junichi Kaburaki,[3] Kazuko Kobayashi,[4] Eiji Matsuura,[4] and Masataka Kuwana[1]

[1]Division of Rheumatology, Department of Internal Medicine, Keio University School of Medicine, Tokyo; [2]Department of Environmental Immuno-dermatology, Yokohama City University Graduate School of Medicine, Yokohama; [3]Department of Internal Medicine, Tokyo Electric Power Company Hospital, Tokyo; and [4]Department of Cell Chemistry, Okayama University Graduate School of Medicine, Dentistry and Pharmaceutical Sciences, Okayama, Japan

Antiphospholipid syndrome (APS) is an autoimmune prothrombotic disorder associated with autoantibodies to phospholipid (PL)–binding proteins, such as β_2-glycoprotein I (β_2GPI). We have recently reported that binding of β_2GPI to anionic PL facilitates processing and presentation of the cryptic β_2GPI epitope that activates pathogenic autoreactive T cells. To clarify mechanisms that induce sustained presentation of the dominant antigenic β_2GPI determinant in patients with APS, T-cell proliferation induced by β_2GPI-treated phosphatidylserine liposome (β_2GPI/PS) was evaluated in bulk peripheral blood mononuclear cell cultures. T cells from patients with APS responded to β_2GPI/PS in the presence of immunoglobulin G (IgG) anti-β_2GPI antibodies derived from APS plasma, and this response was completely inhibited either by the depletion of monocytes or by the addition of anti-FcγRI antibody. These findings indicate that efficient presentation of the cryptic determinants can be achieved by monocytes undergoing FcγRI-mediated uptake of β_2GPI-bound anionic surfaces in the presence of IgG anti-β_2GPI antibodies. Finally, β_2GPI-bound oxidized LDL or activated platelets also induced the specific T-cell response. Continuous exposure to these anionic surfaces may play a critical role in maintaining the pathogenic anti-β_2GPI antibody response in patients with APS. (Blood. 2007;110:4312-4318)

Introduction

Antiphospholipid syndrome (APS) is an autoimmune disorder characterized by arterial and venous thrombosis as well as recurrent intrauterine fetal loss in the presence of antiphospholipid antibodies.[1] β_2-glycoprotein I (β_2GPI) is the most common antigenic target recognized by the antiphospholipid antibodies, and anti-β_2GPI antibodies are shown to be strongly associated with thrombosis and other clinical manifestations of APS.[2-4] β_2GPI is a plasma protein that binds various anionic substances, including phospholipids (PLs), lipoproteins, and activated platelets and endothelial cells.[5-7] Several lines of evidence accumulated from animal models suggest that anti-β_2GPI antibodies are directly involved in the pathogenic processes of APS.[8,9]

We have recently identified $CD4^+$ T cells responsive to β_2GPI in patients with APS.[10-12] β_2GPI-reactive T cells can promote production of pathogenic immunoglobulin G (IgG) anti-β_2GPI antibodies from autologous B cells in vitro. These T cells respond to bacterially expressed recombinant β_2GPI fragments and chemically reduced β_2GPI, but fail to respond to native β_2GPI,[10] indicating that the epitopes recognized by β_2GPI-reactive T cells are cryptic determinants that are not generated through processing of native β_2GPI under normal circumstances. One of the major cryptic determinants recognized by β_2GPI-reactive T cells is the region spanning amino acids (AAs) 276-290, which contains the major PL-binding site at AA 281-288,[13,14] in the context of HLA-DRB4*0103 (DR53).[11] In our recent study employing β_2GPI-reactive $CD4^+$ T-cell clones generated from patients with APS, dendritic cells or macrophages pulsed with β_2GPI-bound phosphatidylserine (PS) liposome induced a response of T-cell clones specific for a peptide encoding AA 276–290 (p276-290) in HLA-DR–restricted and antigen-processing–dependent manners. In contrast, those pulsed with β_2GPI or PS liposome alone failed to induce a response.[15] Together these findings indicate that specialized antigen-presenting cells (APCs) capturing β_2GPI-coated anionic PLs efficiently present a disease-relevant cryptic T-cell determinant of β_2GPI as a result of antigen processing.

In patients with APS, anti-β_2GPI antibody levels are usually stable for many years. However, it remains unclear what mechanisms are responsible for the sustained presentation of the dominant cryptic β_2GPI determinant that activates β_2GPI-reactive T cells to subsequently produce pathogenic anti-β_2GPI antibodies. To elucidate these mechanisms, we examined the cellular and molecular factors required for the sustained activation of β_2GPI-reactive T cells in patients with APS.

Patients, materials, and methods

Patients and controls

This study examined 5 patients, and all fulfilled the revised Sapporo criteria for APS proposed by the International Workshop.[16] These patients were selected based on the presence of DRB4*0103 (DR53), which is known to present a p276-290 peptide to T cells,[11] and positive IgG anti-β_2GPI antibody. The HLA class II alleles, including DRB1 and DRB4, were determined by restriction fragment length polymorphisms combined with

Submitted July 9, 2007; accepted August 23, 2007. Prepublished online as *Blood* First Edition paper, August 28, 2007; DOI 10.1182/blood-2007-07-100008.

An Inside *Blood* analysis of this article appears at the front of this issue.

The publication costs of this article were defrayed in part by page charge payment. Therefore, and solely to indicate this fact, this article is hereby marked "advertisement" in accordance with 18 USC section 1734.

locus-specific polymerase chain reaction using peripheral blood granulocyte-derived genomic DNA as a template.[17] IgG anti-β_2GPI antibody levels were measured with a commercial enzyme-linked immunosorbent assay (ELISA) kit (Yamasa, Choshi, Japan) using immobilized β_2GPI-cardiolipin complex as an antigen source. A commercial kit based on Russell viper venom test (Gradipore, Sydney, Australia) was used to determine the presence of lupus anticoagulant. At the time of blood examination, all the patients were taking low-dose corticosteroids (< 10 mg/day) and low-dose aspirin. Peripheral blood from healthy volunteers was also used as a control source of plasma. All samples were obtained after the patients and control subjects gave their written informed consent in accordance with the Declaration of Helsinki. The study protocol was approved by Keio University International Review Board.

Antigen preparations

Human β_2GPI was purified from normal pooled plasma,[18] and reduced β_2GPI was prepared by incubating β_2GPI with dithiothreitol as previously described.[10] We generated a panel of recombinant maltose-binding protein (MalBP) fusion proteins expressing full-length β_2GPI (GP-F), domains I and II (GP1), domains III and IV (GP2), and domains IV and V (GP3).[10] MalBP alone was prepared as a control antigen. Two 15-mer peptides, p276-290 and a peptide encoding AA 306–320 of human β_2GPI (p306-320), were synthesized using a solid-phase multiple synthesizer (Advanced ChemTech, Louisville, KY).[11]

Liposome containing bovine brain-derived PS (Sigma, St Louis, MO), with a composition of dioleoylphosphatidylcholine (Avanti Polar Lipids, Alabaster, AL) at a molar ratio of 3:7, was prepared and adjusted to a final concentration of 1 μmol/mL.[19,20] Low density lipoprotein (LDL) was isolated from freshly prepared normal human plasma by ultracentrifugation, and oxidized LDL (oxLDL) was prepared by incubating LDL with 5 μM $CuSO_4$ for 8 hours at 37°C.[20] LDL and oxLDL were adjusted to 100 μg/mL of apoB equivalent. Human platelets were separated from platelet-rich plasma using a modified gel filtration method[21] to minimize their activation during an isolation procedure. Resting platelets were then activated by incubation with bovine thrombin (1 U/mL; Mochida, Tokyo, Japan) for 15 minutes. All preparations were incubated with or without native β_2GPI (100 μg/mL) for 30 minutes at room temperature immediately prior to use in the cultures.

Cell preparations

Peripheral blood mononuclear cells (PBMCs) were isolated from heparinized venous blood by Lymphoprep (Fresenius Kabi Norge AS, Oslo, Norway) density-gradient centrifugation. In some experiments, PBMCs were depleted of $CD14^+$ monocytes or $CD19^+$ B cells by incubation with anti-CD14 or anti-CD19 monoclonal antibody (mAb)–coupled magnetic beads (Miltenyi Biotech, Bergisch Gladbach, Germany), respectively, followed by magnetic cell sorting column separation according to the manufacturer's protocol.

Preparation and depletion of IgG from plasma

The IgG fraction was purified or depleted from plasma samples using HiTrap protein G (Amersham Biosciences, Uppsala, Sweden) as described previously.[22] Purity of IgG fractions was confirmed to be more than 95% by sodium dodecyl sulfate–polyacrylamide gel electropheresis, followed by densitometry on Coomassie blue–stained gels. In some experiments, purified IgG was treated with pepsin to prepare $F(ab')_2$ using a Fab2 preparation kit (Pierce Biotechnology, Rockford, IL). We also prepared IgG fractions depleted of antibodies specific to β_2GPI. Briefly, purified IgG samples were treated 3 times with cardiolipin-coated 96-well immunoplates (Nunc F96Maxisorp, Roskilde, Denmark), which were preincubated with β_2GPI or phosphate-buffer saline for 30 minutes. The supernatants were then collected as anti-β_2GPI antibody–depleted or mock-treated IgG. Removal of anti-β_2GPI antibody was confirmed by complete loss of antibody reactivity on the anti-β_2GPI antibody ELISA.

Assays for antigen-specific T-cell response

Antigen-specific T-cell proliferation in the primary cultures was assayed as described previously[10] with some modifications. Briefly, PBMCs (10^5/well) were cultured with or without antigen in 96-well flat-bottomed culture plates for 7 days. RPMI 1640 supplemented with either 10% fetal bovine serum (FBS; JRH Bioscience, Lenexa, KS) or 8% platelet-poor plasma, which was derived from patients with APS and healthy donors, was used as medium. Prior to use, FBS and plasma samples were heat-inactivated and depleted of β_2GPI by passing the samples through a HiTrap Heparin column (Amersham Biosciences) twice, to eliminate the potential influence of intrinsic β_2GPI on the generation of the antigenic peptides. ^{3}H-thymidine (0.5 μCi [0.0185 MBq]/well) was added to the cultures during the final 16 hours. The cells were harvested, and ^{3}H-thymidine incorporation was measured in a Top-Count microplate scintillation counter (Packard, Meriden, CT). Native β_2GPI, reduced β_2GPI, GP-F, GP1, GP2, GP3, and MalBP were used as antigens at a concentration of 10 μg/mL. In addition, PS liposome (0.1 μmol/mL), LDL, oxLDL (10 μg/mL apoB equivalent), resting platelets, or activated platelets (10^6/well) were added to the cultures, with or without preincubation with β_2GPI. To exclude nonspecific unresponsiveness of T cells, all experiments included a culture with phytohemagglutinin at a final concentration of 1 μg/mL. In some experiments, purified IgG, $F(ab')_2$, or anti-β_2GPI antibody–depleted or mock-treated IgG was added at the initiation of the culture. Anti-FcγRI (clone 10.1; R&D Systems, Minneapolis, MN), anti-HLA-DR (clone L243; Leinco Technologies, Baldwin, MO), or isotype-matched control mAb was also added to the culture at a final concentration of 2.5 μg/mL. All experiments were carried out in duplicate or triplicate, and the values are the mean counts per minute (cpm) plus or minus the standard deviation of multiple determinations. In some instances, a T-cell response specific to β_2GPI-treated PS liposome (β_2GPI/PS) was expressed as the ratio of cpm in the culture with β_2GPI/PS to cpm in the culture with PS liposome alone.

Secondary stimulation of peripheral blood T cells was also performed as described.[10] PBMCs were primed with β_2GPI/PS in medium supplemented with 8% autologous plasma for 10 days. Viable cells were then cultured for an additional 3 days in the presence of 50 U/mL recombinant interleukin-2 (Biogen Idec, San Diego, CA) and irradiated (3000 rad) autologous monocyte-derived dendritic cells in medium supplemented with 10% FBS in the absence or presence of β_2GPI, reduced β_2GPI, GP-F, GP1, GP2, GP3, MalBP (10 μg/mL), p276-290, or p306-320 (5 μg/mL). Frequencies of β_2GPI-reactive T cells in peripheral blood T cells were estimated by limiting dilution analysis using GP-F as an antigen.[23] The recognition of p276-290 by peripheral blood T cells was determined based on the specific response to p276-290 by at least 2 T-cell clones established by repeated stimulation of peripheral blood T cells with GP-F.[11]

Results

Clinical and immunologic characteristics of patients with APS

As shown in Table 1, all patients with APS had thrombosis and/or loss of pregnancy, and were positive for lupus anticoagulant. IgG anti-β_2GPI antibody titer was high in all but one patient (APS1). Frequencies of β_2GPI-reactive T cells were variable among patients, and ranged from 2.9 to 12.4 per 10^4 peripheral blood T cells. In addition, T-cell recognition of p276-290 was detected in all 3 patients examined.

T-cell response induced by β_2GPI/PS in PBMC cultures

We first examined the responses of peripheral blood T cells to β_2GPI/PS using regular medium supplemented with FBS (Figure 1A). T cells from all 5 patients responded to GP-F, but failed to proliferate in the presence of β_2GPI/PS. Interestingly, a T-cell response to β_2GPI/PS, as well as to GP-F, was detected when a patient's autologous plasma was used instead of FBS to supplement the culture medium. This response was blocked by anti–HLA-DR

Table 1. Clinical and immunologic characteristics of patients with APS analyzed in this study

Patient no.	Age/sex	Thrombosis	Loss of pregnancy	IgG anti-β_2GPI antibodies (U/mL)†	HLA class II alleles: DRB1	Frequency of β_2GPI-reactive T cells in circulation/10^4 T cells	Recognition of p276–290 by peripheral blood T cells
APS1	51/F	None	+	16	*1502/*0405	4.5	NT
APS2	43/F	DVT, stroke	+	>120	*0405/*1202	2.9	NT
APS3	46/F	DVT, PE, retinal artery thrombosis	+	>120	*1502/*0901	6.8	+
APS4	47/F	Stroke	+	>120	*1501/*0403	8.1	+
APS9	46/F	DVT, PE, stroke, amaurosis fugax	NA	>120	*0901	12.4	+

All patients were lupus anticoagulant positive; all DRB4 alleles were *0103.
DVT indicates deep venous thrombosis of lower extremity; PE, pulmonary embolism; NA, not applicable; and NT, not tested.
†Normal range less than 3.5 U/mL.

mAb, but not by control mAb (data not shown). However, a β_2GPI/PS-induced response was not detected in the culture with allogenic plasma from a healthy individual. This finding was reproducible in a total of 7 PBMC samples obtained from 5 patients with APS.

Next, PBMCs from a patient with APS were cultured with β_2GPI/PS or PS liposome alone in medium supplemented with 2 different lots of FBS, plasma samples from 4 patients with APS, or samples from 3 healthy donors (Figure 1B). The β_2GPI/PS-specific response was exclusively detected in cultures with autologous and allogenic plasmas derived from patients with APS, although the degree of response was variable among APS plasmas. Analogous findings were obtained with PBMCs from 3 additional patients with APS. In all cases, the lowest response was detected in the culture supplemented with APS1 plasma, which contained low-titer anti-β_2GPI antibodies.

We next sought to confirm whether T-cell responses induced by β_2GPI/PS in cultures with APS plasma were specific to β_2GPI. Peripheral blood T cells primed with β_2GPI/PS in medium supplemented with autologous plasma were further examined for their reactivity to various β_2GPI preparations in the secondary culture with FBS (Figure 2). β_2GPI/PS-primed T cells from all 5 patients specifically responded to reduced β_2GPI, GP-F, and GP3, indicating a specific recognition of β_2GPI-derived peptides. More important, the cryptic p276-290 was efficiently presented by APCs in culture with β_2GPI/PS and APS plasma. T-cell recognition of GP1 was detected in APS2, APS4, and APS9 samples, whereas recognition of GP2 was detected in APS3 and APS9. Taken together, these findings together indicate that a soluble factor(s) contained in plasma from patients with APS, but not in FBS or plasma from healthy individuals, plays an essential role in activation of β_2GPI-specific T cells in bulk PBMC cultures with β_2GPI/PS.

IgG anti-β_2GPI autoantibody as an essential factor for T-cell recognition of β_2GPI/PS

Since the degree of the β_2GPI/PS-specific T-cell response appeared to correlate with IgG anti-β_2GPI antibody titers, we hypothesized that IgG anti-β_2GPI antibodies in APS plasma are required for peripheral blood T cells to respond to β_2GPI/PS. To test this hypothesis, we first prepared IgG-depleted APS plasma samples to evaluate the β_2GPI/PS-induced T-cell response (Figure 3A). Depletion of IgG from APS plasma resulted in complete loss of the β_2GPI/PS-induced T-cell response, but addition of autologous IgG back to the IgG-depleted APS plasma restored the response in a dose-dependent fashion. In contrast, addition of IgG prepared from healthy plasma had no effect (data not shown). Interestingly, β_2GPI/PS-induced T-cell response was also detected in medium supplemented with healthy plasma in the presence of IgG derived from APS plasma. This response was abolished when F(ab')$_2$ was used instead of intact IgG, indicating an important role of the Fc portion of IgG.

We further examined the effects of depletion of β_2GPI-specific antibody on the β_2GPI/PS-induced T-cell response in PBMC cultures with APS IgG (Figure 3B). β_2GPI/PS-induced T-cell

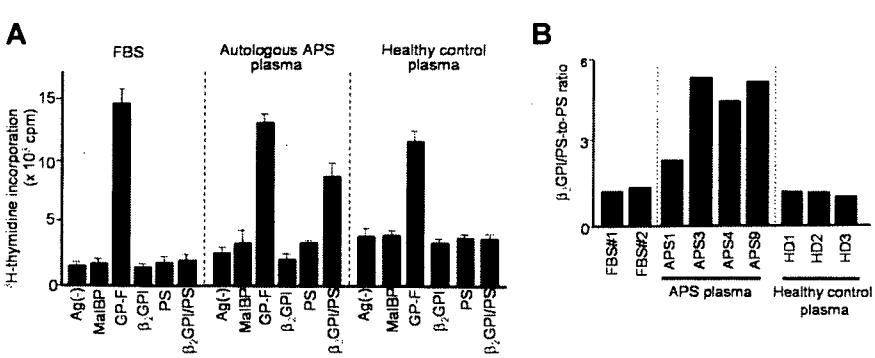

Figure 1. T-cell response to β_2GPI/PS in bulk PBMC cultures supplemented with FBS, autologous APS plasma, or healthy control plasma. (A) PBMCs from APS4 were cultured in triplicate with or without antigens, including MalBP, GP-F, β_2GPI, PS, and β_2GPI/PS, in medium supplemented with FBS, autologous APS plasma, or healthy control plasma. The antigen-induced T-cell proliferative response was assessed by ^{3}H-thymidine incorporation. Results are shown as mean (column) and standard deviation (error bar) of triplicate measurements. Analogous findings were obtained in 7 independent experiments in PBMCs from all 5 patients with APS. (B) β_2GPI/PS-specific T-cell response in PBMC cultures of APS4 in medium supplemented with 2 different lots of FBS (no. 1 and no. 2), plasma samples from 4 APS patients (APS1, 3, 4, and 9), or plasma samples from 3 healthy donors (HD1, 2, and 3). β_2GPI/PS-specific T-cell response was expressed as a β_2GPI/PS-to-PS ratio, which was the mean cpm incorporated in the triplicate culture with β_2GPI/PS divided by the mean cpm incorporated in the triplicate culture with PS alone (standard deviations for the individual results were within 20% of the mean in all cases). Similar results were obtained from 3 additional patients with APS (APS1, APS3, and APS9).

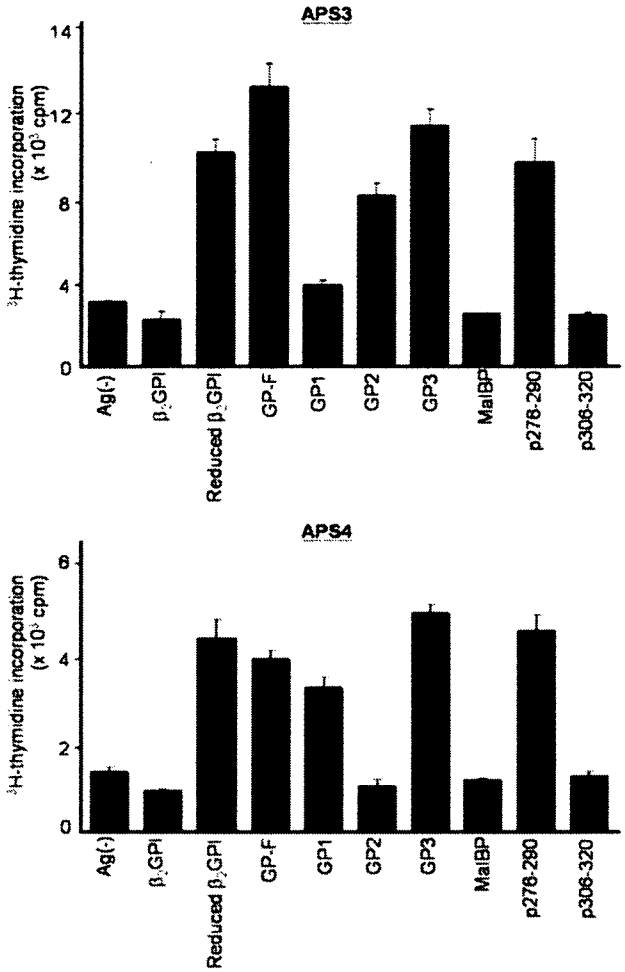

Figure 2. Proliferative responses of β_2GPI/PS-primed T cells to various β_2GPI preparations in secondary cultures. PBMCs from APS3 (top) and APS4 (bottom) were stimulated with β_2GPI/PS for 10 days in medium supplemented with autologous plasma. The viable T cells were then cultured in duplicate with β_2GPI, reduced β_2GPI, GP-F, GP1, GP2, GP3, MalBP, p276-290, or p306-320 in medium containing FBS. After 3 days, ^{3}H-thymidine incorporation was measured. Results are shown as mean (column) and standard deviation (error bar) of duplicate measurements.

response was detected in the presence of mock-treated APS IgG, but completely abolished by depletion of β_2GPI-reactive IgG. These findings indicate that IgG anti-β_2GPI antibodies are required for the T cells of patients with APS to respond to β_2GPI/PS in bulk PBMC cultures.

Roles of β_2GPI/PS-containing immune complex in β_2GPI/PS-induced T-cell response

Since anti-β_2GPI antibodies in sera from patients with APS recognize β_2GPI/PS,[20] it is likely that β_2GPI/PS is readily opsonized by IgG anti-β_2GPI antibodies in culture with APS plasma. To evaluate which APCs contained in PBMCs capture this immune complex to induce a specific T-cell response to β_2GPI peptides, we analyzed PBMCs depleted of CD14$^+$ monocytes, CD19$^+$ B cells, or mock-treated in cultures with β_2GPI/PS and autologous plasma (Figure 4A). The β_2GPI/PS-induced T-cell response was completely inhibited by depletion of monocytes, but was partially suppressed by depletion of B cells, suggesting a primary role of monocytes in our system.

We further evaluated the potential involvement of Fcγ receptors in recognition of the immune complex by monocytes, as the anti-β_2GPI F(ab')$_2$ was incapable of inducing the T-cell response to β_2GPI/PS. The β_2GPI/PS-induced T-cell response was completely blocked by anti-FcγRI mAb, but not by control mAb (Figure 4B). Together these findings indicate that efficient β_2GPI/PS-induced T-cell response is achieved by monocytes undergoing FcγRI-mediated uptake of β_2GPI/PS opsonized by IgG anti-β_2GPI autoantibodies.

T-cell response to β_2GPI-treated oxLDL and platelet microparticles

PS liposomes were chemically synthesized, and may not be relevant to patients with APS in vivo. To examine whether anionic substances present in the circulation, such as oxLDL or platelet microparticles, can substitute for PS liposomes in inducing the β_2GPI-specific T-cell response, PBMCs from a representative patient with APS were cultured with various anionic and control substances pretreated with or without β_2GPI in medium supplemented with autologous plasma (Figure 5). OxLDL or activated platelets pretreated with β_2GPI induced a T-cell proliferative

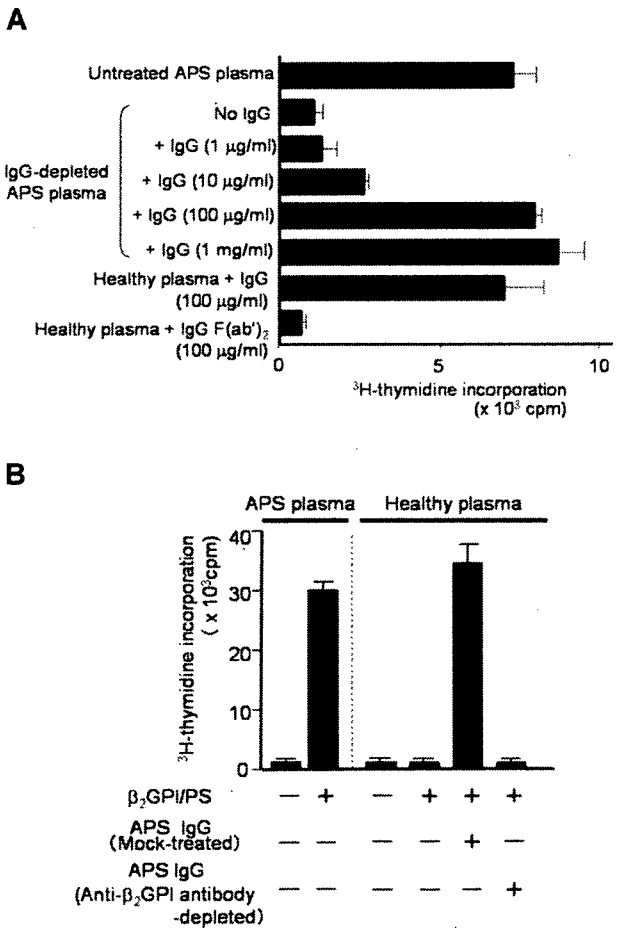

Figure 3. β_2GPI/PS-induced T-cell response in PBMC cultures with or without IgG derived from APS plasma. (A) PBMCs obtained from APS3 were cultured in triplicate with β_2GPI/PS in medium supplemented with untreated or IgG-depleted autologous APS plasma, or healthy plasma. Purified IgG (1 μg/mL-1 mg/mL) or IgG F(ab')$_2$ (100 μg/mL) from APS3 was added to the cultures. After 7 days, the T-cell proliferative response induced by β_2GPI/PS was measured by ^{3}H-thymidine incorporation. Results are shown as mean (column) and standard deviation (error bar). Concordant results were obtained with a sample from APS4. (B) PBMCs derived from APS3 were cultured in triplicate with or without β_2GPI/PS in medium supplemented with autologous APS plasma or healthy plasma. An anti-β_2GPI antibody–depleted or mock-treated autologous IgG fraction was added to the initiation of cultures. After 7 days, the T-cell proliferative response was measured by ^{3}H-thymidine incorporation. Results are shown as mean (column) and standard deviation (error bar). Concordant results were obtained with a sample from APS4.

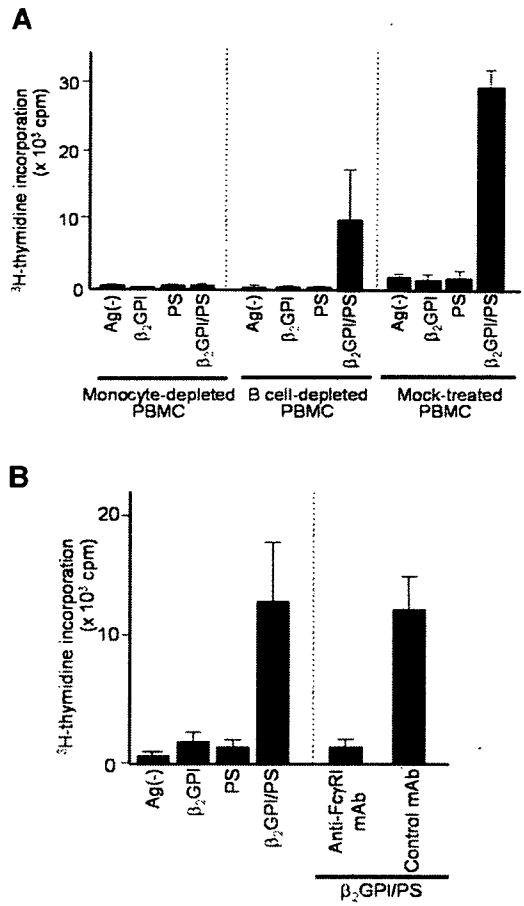

Figure 4. Effects of APC depletion or anti-FcγRI mAb on β_2GPI/PS-induced T-cell response. (A) CD14$^+$ monocyte-depleted, CD19$^+$ B-cell–depleted, and mock-treated PBMCs derived from APS3 were cultured for 7 days with or without β_2GPI, PS, or β_2GPI/PS in medium supplemented with autologous APS plasma, and the T-cell proliferative response was measured by ^{3}H-thymidine incorporation. Results are shown as mean (column) and standard deviation (error bar) of duplicate measurements. Analogous results were obtained in a total of 4 independent experiments using samples from 3 patients with APS (APS1, APS3, and APS4). (B) PBMCs from APS2 were cultured for 7 days with or without β_2GPI, PS, or β_2GPI/PS in medium supplemented with autologous APS plasma. Anti-FcγRI or isotype-matched control mAb was added to the initiation of cultures. The T-cell proliferative response was evaluated by ^{3}H-thymidine incorporation. Results are shown as mean (column) and standard deviation (error bar) of duplicate measurements. Concordant results were obtained with samples from 3 patients with APS (APS2, APS3, and APS9).

response, as observed in cultures with β_2GPI/PS. These responses were specifically inhibited by anti–HLA-DR mAb (data not shown). Thus, oxLDL and activated platelets can be in vivo sources of anionic surfaces that bind β_2GPI and promote the efficient presentation of β_2GPI cryptic peptides by APCs.

Discussion

This study evaluated the potential cellular and molecular mechanisms that induce sustained presentation of the dominant cryptic β_2GPI determinant that activates β_2GPI-reactive T cells to subsequently produce pathogenic anti-β_2GPI antibodies in patients with APS. Here we demonstrate that efficient presentation of cryptic determinants recognized by β_2GPI-reactive T cells is achieved by monocytes undergoing FcγRI-mediated uptake of β_2GPI/PS opsonized by IgG anti-β_2GPI antibodies. High avidity IgG anti-β_2GPI antibodies, which were reported to possess high pathogenicity,[24] would also have enhanced capacity to promote this process. We

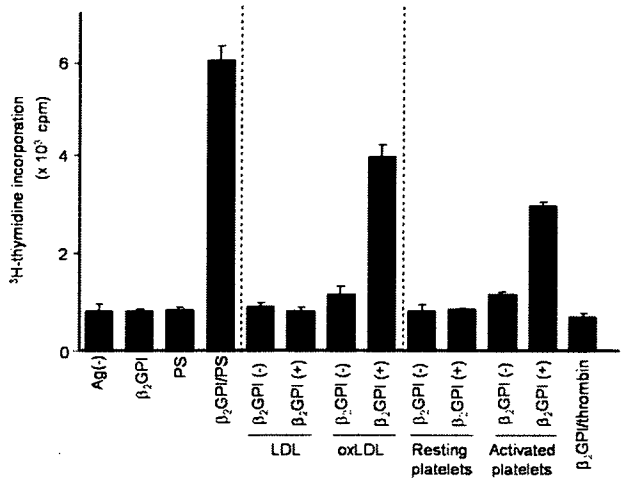

Figure 5. T-cell responses to β_2GPI-treated anionic substances present in circulation. PBMCs from APS4 were cultured with or without various antigen preparations in medium supplemented with autologous APS plasma. Antigens used included β_2GPI alone, as well as PS, LDL, oxLDL, resting platelets, and activated platelets, which were treated either with or without β_2GPI. Thrombin, which was used to activate platelets, in combination with β_2GPI served as a control. T-cell proliferative response was measured by ^{3}H-thymidine incorporation. Results are shown as mean (column) and standard deviation (error bar) of duplicate measurements. Analogous results were obtained in samples from all 5 patients with APS.

propose a model by which a pathogenic loop maintains sustained anti-β_2GPI autoantibody production in patients with APS (Figure 6). This model consists of 3 major players: β_2GPI-reactive CD4$^+$ T cells, anti-β_2GPI antibody-producing B cells, and macrophages. Upon recognition of β_2GPI cryptic peptides, such as p276-290, presented by macrophages in the context of HLA-DR, β_2GPI-reactive CD4$^+$ T cells are activated and exert helper activity that induces IgG anti-β_2GPI antibody production from B cells. This process can be achieved by T-B cell collaboration through CD40-CD154 engagement and T cell–derived IL-6.[11] IgG anti-β_2GPI antibodies subsequently recognize β_2GPI-bound anionic surfaces in circulation, resulting in enhanced phagocytosis of this immune

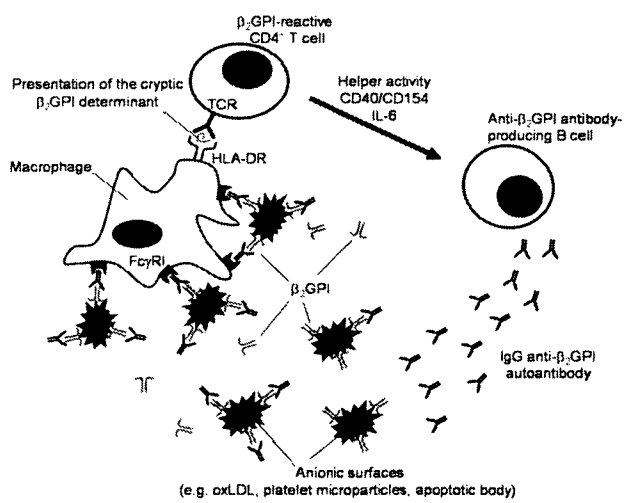

Figure 6. A schematic model representing a continuous autoimmune loop carried out by macrophage, β_2GPI-reactive CD4$^+$ T cell, and anti-β_2GPI antibody–producing B cell. The macrophage efficiently presents the cryptic β_2GPI determinant in the context of HLA-DR. The β_2GPI-reactive CD4$^+$ T cell is activated by recognition of the cryptic β_2GPI peptide and exerts helper activity that induces production of IgG anti-β_2GPI autoantibodies from the specific B cell. The immune complex consisting of anionic surfaces, β_2GPI, and IgG anti-β_2GPI antibodies were captured by macrophages via FcγRI.

complex by macrophages through FcγRI. In this regard, it has been shown that anti-β_2GPI antibodies in APS sera are predominantly of IgG2 subclass,[25,26] which has low affinity to FcγRI. However, anti-β_2GPI antibodies of IgG1 or IgG3 subclass were also detected in many patients with APS. These low levels of anti-β_2GPI antibodies with high binding affinity to FcγRI may be sufficient to drive the pathogenic loop. We have previously shown that β_2GPI binding to anionic substances promotes the generation of β_2GPI cryptic peptides by protecting the major PL-binding site from protease attack during antigen-processing by dendritic cells or macrophages.[15] Since it has been shown that antibody binding to the antigen boosts the generation of some minor epitopes,[27] binding of IgG anti-β_2GPI antibodies to the β_2GPI-anionic substance complex may further amplify generation of previously cryptic β_2GPI peptides. Moreover, this immune complex is likely to stimulate monocytes via FcγRI to secrete tissue factor, which is shown to play an important role in thrombus formation in patients with APS.[28] Partial suppression of the β_2GPI/PS-induced T-cell response by depletion of B cells in our system suggests that presentation of cryptic β_2GPI peptides could be mediated through B cells that capture β_2GPI/PS via specific B-cell receptors. This process, however, might have less of an impact on the T-cell response, due likely to low abundance of specific B cells recognizing β_2GPI/PS. The mechanism that triggers anti-β_2GPI antibody response in patients with APS remains unclear, but once this autoimmune loop is established, pathogenic anti-β_2GPI antibodies are continuously produced.

The presence of anionic substances with the capacity to bind β_2GPI is essential to drive the pathogenic loop inducing continuous anti-β_2GPI antibody production in patients with APS. Potential anionic substances in the circulation include apoptotic bodies, microparticles derived from activated platelets and endothelial cells, and oxLDL. Since β_2GPI is abundantly present in the circulation (~200 μg/mL), excessive exposure to anionic substances would result in the immediate formation of a complex with β_2GPI. In the present study, we have clearly demonstrated that microparticles derived from activated platelets and oxLDL can function as a substitute for the PS liposome that binds to β_2GPI and facilitates presentation of the cryptic epitopes of β_2GPI as a consequence of antigen processing. In addition, some of our group (E.M. and K.K.) reported that stable and nondissociable β_2GPI-oxLDL complexes were frequently detected in sera from patients with APS and/or systemic lupus erythematosus, but not in healthy individuals.[29] In addition, β_2GPI is known to have antiatherosclerosis activity by preventing oxLDL uptake by macrophages via scavenger receptor, but binding of IgG anti-β_2GPI antibodies to β_2GPI-oxLDL complexes mediates atherosclerosis by promoting phagocytosis of macrophages via Fcγ receptor.[29-31] Furthermore, elevated levels of procoagulant microparticles were detected in patients with APS in association with anti-β_2GPI antibodies and lupus anticoagulant.[32-34] The presence of a large quantity of anionic substances in circulation in patients with APS supports our proposed model.

Based on our model, therapeutic strategies that inhibit pathogenic anti-β_2GPI antibody production should target interrupting the continuous autoimmune loop carried out by macrophages and β_2GPI-reactive $CD4^+$ T cells and B cells. These immune cells are already targets of therapies under consideration, such as the anti-CD20 chimeric antibody rituximab.[35] Another potential therapeutic approach includes the removal of immune complexes consisting of β_2GPI, anionic substance, and anti-β_2GPI antibodies. Accordingly, plasma exchange and double filtration plasmapheresis, which theoretically remove such immune complexes, are shown to be effective for patients with intractable APS, including catastrophic APS.[36,37] Alternatively, small molecules that inhibit Fc receptor downstream signaling would have beneficial effects in patients with APS by suppressing the generation of β_2GPI cryptic peptides.[38]

In summary, excessive exposure to anionic surfaces may play a key role in maintaining the pathogenic anti-β_2GPI antibody response in patients with APS. Further studies should focus on mechanisms that prime the autoimmune loop and development of novel therapeutic strategies targeting the pathogenic process.

Acknowledgments

We thank Yuka Okazaki and Takahide Arai for expert technical assistance.

This work was supported by a grant from the Japanese Ministry of Health, Welfare, and Labor, and a Grant-in-Aid for Scientific Research from the Japanese Ministry of Education, Science, Sports and Culture.

Authorship

Contribution: Y.Y., N.S., J.K., K.K., and E.M. performed experiments; Y.Y. and M.K. analyzed results and made the figures; Y.Y. and M.K. designed the research and wrote the paper.

Conflict-of-interest disclosure: The authors declare no competing financial interests.

Correspondence: Masataka Kuwana, Division of Rheumatology, Department of Internal Medicine, Keio University School of Medicine, 35 Shinanomachi, Shinjuku-ku, Tokyo 160-8582, Japan; e-mail: kuwanam@sc.itc.keio.ac.jp.

References

1. Harris EN, Chan JK, Asherson RA, Aber VR, Gharavi AE, Hughes GRV. Thrombosis, recurrent fetal loss, and thrombocytopenia: predictive value of the anticardiolipin antibody test. Arch Intern Med. 1986;146:2153-2156.
2. McNeil HP, Simpson RJ, Chesterman CN, Krilis SA. Antiphospholipid antibodies are directed against a complex antigen that includes a lipid-binding inhibitor of coagulation: β_2-glycoprotein I (apolipoprotein H). Proc Natl Acad Sci U S A. 1990;87:4120-4124.
3. Galli M, Comfurius P, Maassen C, et al. Anticardiolipin antibodies (ACA) directed not to cardiolipin but to a plasma protein cofactor. Lancet. 1990;335:1544-1547.
4. Cabral AR, Amigo MC, Cabiedes J, Alarcon-Segovia D. The antiphospholipid/cofactor syndromes: a primary variant with antibodies to β_2-glycoprotein-I but no antibodies detectable in standard antiphospholipid assays. Am J Med. 1996;101:472-481.
5. Wurm H. β_2-glycoprotein I (apolipoprotein H) interactions with phospholipid vesicles. Int J Biochem. 1984;16:511-515.
6. Shi W, Chong BH, Chesterman CN. β_2-glycoprotein I is a requirement for anticardiolipin antibodies binding to activated platelets: differences with lupus anticoagulant. Blood. 1993;81:1255-1262.
7. Del Papa N, Guidali L, Sala A, et al. Endothelial cells as target for antiphospholipid antibodies: human polyclonal and monoclonal anti β_2-glycoprotein I antibodies react in vitro with endothelial cells through adherent β_2-glycoprotein I and induce endothelial activation. Arthritis Rheum. 1997;40:551-561.
8. Blank M, Faden D, Tincani A, et al. Immunization with anticardiolipin cofactor (β_2-glycoprotein I) induces experimental antiphospholipid syndrome in naive mice. J Autoimmun. 1994;7:441-455.
9. Levy Y, Ziporen L, Gilburd B, et al. Membranous nephropathy in primary antiphospholipid syndrome: description of a case and induction of renal injury in SCID mice. Hum Antibodies Hybridomas. 1996;7:91-96.

10. Hattori N, Kuwana M, Kaburaki J, Mimori T, Ikeda Y, Kawakami Y. T cells that are autoreactive to β_2-glycoprotein I in patients with antiphospholipid syndrome and healthy individuals. Arthritis Rheum. 2000;43:65-75.
11. Arai T, Yoshida K, Kaburaki J, et al. Autoreactive CD4+ T-cell clones to β_2-glycoprotein I in patients with antiphospholipid syndrome: preferential recognition of the major phospholipid-binding site. Blood. 2001;98:1889-1896.
12. Yoshida K, Arai T, Kaburaki J, Ikeda Y, Kawakami Y, Kuwana M. Restricted T-cell receptor β-chain usage by T cells autoreactive to β_2-glycoprotein I in patients with antiphospholipid syndrome. Blood. 2002;99:2499-2504.
13. Hunt J, Krilis SA. The fifth domain of β_2-glycoprotein I contains a phospholipid binding site (Cys281-Lys288) and a region recognized by anticardiolipin antibodies. J Immunol. 1994;152:653-659.
14. Sheng Y, Sali A, Herzog H, Lahnstein J, Krilis SA. Site-directed mutagenesis of recombinant human β_2-glycoprotein I identifies a cluster of lysine residues that are critical for phospholipid binding and anti-cardiolipin antibody activity. J Immunol. 1996; 157:3744-3751.
15. Kuwana M, Matsuura S, Kobayashi K, et al. Binding of β_2-glycoprotein I to anionic phospholipids facilitates processing and presentation of a cryptic epitope that activates pathogenic autoreactive T cells. Blood. 2005;105:1552-1557.
16. Miyakis S, Lockshin MD, Atsumi T, et al. International consensus statement on an update of the classification criteria for definite antiphospholipid syndrome (APS). J Thromb Haemost. 2006;4: 295-306.
17. Naruse T, Ando R, Nose Y, et al. HLA-DRB4 genotyping by PCR-RFLP: diversity in the associations between HLA-DRB4 and DRB1 alleles. Tissue Antigens. 1997;49:152-159.
18. Matsuura E, Igarashi Y, Fujimoto M, et al. Heterogeneity of anticardiolipin antibodies defined by the anticardiolipin cofactor. J Immunol. 1992;148: 3885-3891.
19. Liu Q, Kobayashi K, Furukawa J, et al. ω-Carboxyl variants of 7-ketocholesteryl esters are ligands for β_2-glycoprotein I and mediate antibody-dependent uptake of oxidized LDL by macrophages. J Lipid Res. 2002;43:1486-1495.
20. Kobayashi K, Matsuura E, Liu Q, et al. A specific ligand for β_2-glycoprotein I mediates autoantibody-dependent uptake of oxidized low density lipoprotein by macrophages. J Lipid Res. 2001; 42:697-709.
21. Bogdan W, Urszula K, Lidia M, et al. Comparison of platelet aggregability and P-selectin surface expression on platelets isolated by different methods. Thromb Res. 2000;99:495-502.
22. Nakamura M, Tanaka Y, Satoh T, et al. Autoantibody to CD40 ligand in systemic lupus erythematosus: association with thrombocytopenia but not thromboembolism. Rheumatology (Oxford). 2006;45: 150-156.
23. Kuwana M, Okazaki Y, Kaburaki J, et al. Spleen is a primary site for activation of platelet-reactive T and B cells in patients with immune thrombocytopenic purpura. J Immunol. 2002;168:3675-3682.
24. Božič B, Čučnik T, Kveder T, Rozman B. Avidity of anti-beta-2-glycoprotein I antibodies. Autoimmunity Rev. 2005;4:303-308.
25. Samarkos M, Davies KA, Gordon C, Walport MJ, Loizou S. IgG subclass distribution of antibodies against β_2-GPI and cardiolipin in patients with systemic lupus erythematosus and primary antiphospholipid syndrome, and their clinical associations. Rheumatology (Oxford). 2001;40:1026-1032.
26. Amengual O, Atsumi T, Khamashta MA, Bertolaccini ML, Hughes GRV. IgG2 restriction of anti-β_2-glycoprotein I as the basis for the association between IgG2 anticardiolipin antibodies and thrombosis in the antiphospholipid syndrome. Arthritis Rheum. 1998;41:1513-1514.
27. Simitsek PD, Campbell DG, Lanzavecchia A, Fairweather N, Watts C. Modulation of antigen processing by bound antibodies can boost or suppress class II major histocompatibility complex presentation of different T cell determinants. J Exp Med. 1995;181:1957-1963.
28. Wolberg AS, Roubey RAS. Mechanisms of autoantibody-induced monocyte tissue factor expression. Thromb Res. 2004;114:391-396.
29. Kobayashi K, Kishi M, Atsumi T, et al. Circulating oxidized LDL forms complexes with β_2-glycoprotein I: implication as an atherogenic autoantigen. J Lipid Res. 2003;44:716-726.
30. Matsuura E, Kobayashi K, Koike T, Shoenfeld Y. Autoantibody-mediated atherosclerosis. Autoimmunity Rev. 2002:1:348-353.
31. Shoenfeld A, Gerli R, Doria A, et al. Accelerated atherosclerosis in autoimmune rheumatic diseases. Circulation. 2005;112:3337-3347.
32. Morel O, Jesel L, Freyssinet JM, Toti F. Elevated levels of procoagulant microparticles in a patient with myocardial infarction, antiphospholipid antibodies and multifocal cardiac thrombosis. Thromb J. 2005;3:15.
33. Ambrozic A, Bozic B, Kveder T, et al. Budding, vesiculation and permeabilization of phospholipid membranes-evidence for a feasible physiologic role of beta2-glycoprotein I and pathogenic actions of anti-beta2-glycoprotein I antibodies. Biochim Biophys Acta. 2005;1740:38-44.
34. Combes V, Simon AC, Grau GE, et al. In vitro generation of endothelial microparticles and possible prothrombotic activity in patients with lupus anticoagulant. J Clin Invest. 1999;104:93-102.
35. Rubenstein E, Arkfeld DG, Metyas S, Shinada S, Ehresmann S, Liebman HA. Rituximab treatment for resistant antiphospholipid syndrome. J Rheumatol. 2006;33:355-357.
36. Cervera R, Font J, Gomez-Puerta JA, et al. Validation of the preliminary criteria for the classification of catastrophic antiphospholipid syndrome. Ann Rheum Dis. 2005;64:1205-1209.
37. Otsubo S, Nitta K, Yumura W, Nihei H, Mori N. Antiphospholipid syndrome treated with prednisolone, cyclophosphamide and double-filtration plasmapheresis. Intern Med. 2002;41:725-729.
38. Braselmann S, Taylor V, Zhao H, et al. R406, an orally available spleen tyrosine kinase inhibitor blockes Fc receptor signaling and reduces immune complex-mediated inflammation. J Pharmacol Exp Ther. 2006;319:998-1008.

STEM CELLS
TISSUE-SPECIFIC STEM CELLS

Endothelial Differentiation Potential of Human Monocyte-Derived Multipotential Cells

MASATAKA KUWANA,[a,d] YUKA OKAZAKI,[a] HIROAKI KODAMA,[b] TAKASHI SATOH,[a] YUTAKA KAWAKAMI,[d] YASUO IKEDA[c]

Divisions of [a]Rheumatology, [b]Cardiology, and [c]Hematology, Department of Internal Medicine, and [d]Institute for Advanced Medical Research, Keio University School of Medicine, Tokyo, Japan

Key Words. Endothelial differentiation • Endothelial cells • Monocyte • Vascularization

ABSTRACT

We previously reported a unique $CD14^+CD45^+CD34^+$ type I collagen$^+$ cell fraction derived from human circulating $CD14^+$ monocytes, named monocyte-derived multipotential cells (MOMCs). This primitive cell population contains progenitors capable of differentiating along the mesenchymal and neuronal lineages. Here, we investigated whether MOMCs can also differentiate along the endothelial lineage. MOMCs treated with angiogenic growth factors for 7 days changed morphologically and adopted a caudate appearance with rod-shaped microtubulated structures resembling Weibel-Palade bodies. Almost every cell expressed CD31, CD144, vascular endothelial growth factor (VEGF) type 1 and 2 receptors, Tie-2, von Willebrand factor (vWF), endothelial nitric-oxide synthase, and CD146, but CD14/CD45 expression was markedly downregulated. Under these culture conditions, the MOMCs continued to proliferate for up to 7 days. Functional characteristics, including vWF release upon histamine stimulation and upregulated expression of VEGF and VEGF type 1 receptor in response to hypoxia, were indistinguishable between the MOMC-derived endothelial-like cells and cultured mature endothelial cells. The MOMCs responded to angiogenic stimuli and promoted the formation of mature endothelial cell tubules in Matrigel cultures. Finally, in xenogenic transplantation studies using a severe combined immunodeficient mouse model, syngeneic colon carcinoma cells were injected subcutaneously with or without human MOMCs. Cotransplantation of the MOMCs promoted the formation of blood vessels, and more than 40% of the tumor vessel sections incorporated human endothelial cells derived from MOMCs. These findings indicate that human MOMCs can proliferate and differentiate along the endothelial lineage in a specific permissive environment and thus represent an autologous transplantable cell source for therapeutic neovasculogenesis. STEM CELLS *2006;24: 2733–2743*

INTRODUCTION

Circulating cells derived from bone marrow have been reported to promote the repair of ischemic damage in organs, possibly by inducing and modulating vasculogenesis in ischemic areas or by stimulating the re-endothelialization of injured blood vessels [1, 2]. Several studies have highlighted the contribution to neovasculogenesis in adults of circulating endothelial cell progenitors, which are characterized by the expression of CD34 and vascular endothelial growth factor (VEGF) type 2 receptor (VEGFR2) [3, 4]. Recently, Harraz et al. reported that $CD14^+$ monocytes also have the potential to be incorporated into the endothelium of blood vessels in mouse ischemic limbs and to transdifferentiate into endothelial cells [5]. In addition, recent studies have shown that human $CD14^+$ monocytes coexpress endothelial lineage markers and form cord-like structures in vitro in response to a combination of angiogenic factors [6, 7]. On the other hand, several lines of evidence indicate that endothelial progenitor cells (EPCs) obtained by culturing peripheral blood mononuclear cells (PBMCs) in media favoring endothelial differentiation, which were originally reported as circulating angioblasts [3], are composed predominantly of endothelial-like cells (ELCs) derived from circulating monocytes [8, 9]. These findings indicate a potential developmental relationship between monocytes and endothelial cells and suggest that the monocyte population may be recruited for vasculogenesis and may represent an endothelial precursor population.

Recently, we identified a human cell population termed monocyte-derived multipotential cells (MOMCs; previously termed monocyte-derived mesenchymal progenitors) that has a unique phenotype that is positive for CD14, CD45, CD34, and

Correspondence: Masataka Kuwana, M.D., Ph.D., Division of Rheumatology, Department of Internal Medicine, Keio University School of Medicine, 35 Shinanomachi, Shinjuku-ku, Tokyo 160-8582, Japan. Telephone: 81-3-3350-3567; Fax: 81-3-3350-3567; e-mail: kuwanam@sc.itc.keio.ac.jp Received January 12, 2006; accepted for publication July 27, 2006; first published online in STEM CELLS *EXPRESS* August 3, 2006. 1066-5099/2006/$20.00/0 doi: 10.1634/stemcells.2006-0026

type I collagen [10]. This cell population contains progenitors that can differentiate into several distinct mesenchymal cell types, including bone, cartilage, fat, and skeletal and cardiac muscle cells, as well as neurons [10–12]. MOMCs are generated in vitro by culturing circulating $CD14^+$ monocytes on fibronectin in the presence of soluble factors derived from circulating $CD14^-$ cells. MOMCs express several endothelial markers, including CD144/vascular endothelial (VE)-cadherin and VEGF type 1 receptor (VEGFR1), and have the ability to take up acetylated low-density lipoproteins (AcLDLs). In this study, the endothelial differentiation potential of human MOMCs was examined, and the capacity to induce in vitro and in vivo vascularization was compared between MOMCs and ELCs generated from circulating $CD14^+$ monocytes in the EPC induction culture.

Materials and Methods

Preparation of MOMCs

Human MOMCs were generated from the peripheral blood of healthy adult individuals, as described previously [10]. Briefly, PBMCs were resuspended in low-glucose Dulbecco's modified Eagle's medium (DMEM) supplemented with 10% fetal bovine serum (FBS) (Sigma-Aldrich, St. Louis, http://www.sigmaaldrich.com), 2 mM L-glutamine, 50 U/ml penicillin, and 50 μg/ml streptomycin, spread at a density of 2×10^6 cells per milliliter on plastic plates that had been previously treated with 10 μg/ml human fibronectin (Sigma-Aldrich), incubated overnight at 4°C, and cultured without any additional growth factors at 37°C with 5% CO_2 in a humidified atmosphere. The medium containing floating cells was exchanged with fresh medium every 3 days. After 7–10 days of culture, the adherent cells were collected as MOMCs and used in the following experiments. All blood samples were obtained after the subjects gave their written informed consent, as approved by the Institutional Review Board.

In some experiments, circulating $CD14^+$ monocytes were separated from PBMCs using an anti-CD14 monoclonal antibody (mAb) coupled to magnetic beads (CD14 MicroBeads; Miltenyi Biotec, Bergisch Gladbach, Germany, http://www.miltenyibiotec.com) followed by magnetic cell sorting (MACS) column separation according to the manufacturer's protocol. A fraction enriched in $CD14^+$ cells was also prepared from cultured MOMCs using anti-CD14 mAb-coupled magnetic beads. Flow cytometric analysis revealed that these sorted fractions contained >99% $CD14^+$ cells. MOMCs were generated from the freshly isolated $CD14^+$ monocytes by culturing them alone on fibronectin-coated plates in $CD14^-$ cell-conditioned medium, which was prepared by culturing $CD14^-$ cells on fibronectin-coated plates overnight [10]. PBMCs depleted of $CD34^+$ cells were also prepared, using anti-CD34 mAb-coupled MACS beads, and used in the culture for MOMC differentiation.

Other Cell Types

Macrophages were prepared by culturing adherent PBMCs on plastic plates in Medium 199 (Sigma-Aldrich) supplemented with 20% FBS and 4 ng/ml macrophage-colony stimulating factor (R&D Systems Inc., Minneapolis, http://www.rndsystems.com) for 7 days. Human umbilical vein endothelial cells (HUVECs) and human pulmonary artery endothelial cells (HPAECs) were purchased from Cambrex (Baltimore, http://www.cambrex.com). Primary cultures of human fibroblasts were established from the skin biopsy of a healthy volunteer and maintained in low-glucose DMEM with 10% FBS.

Endothelial Induction Culture

The endothelial induction culture was carried out using the same medium as for the generation of EPCs [8, 9]. Specifically, MOMCs or freshly isolated $CD14^+$ monocytes (40%–50% confluent) were cultured on fibronectin-coated plastic plates or chamber slides for up to 14 days in endothelial cell basal medium-2 (EBM-2) (Clonetics) supplemented with EBM-2 MV SingleQuots containing 5% FBS, VEGF, basic fibroblast growth factor (bFGF), epidermal growth factor, insulin-like growth factor-1, heparin, and ascorbic acid. The medium was exchanged with fresh medium every 3–4 days.

Transmission Electron Microscopy

MOMCs grown in endothelial differentiation or control cultures were immediately fixed with 2.5% glutaraldehyde, postfixed in 2% osmium tetroxide, dehydrated in a series of graded ethanol solutions and propylene oxide, and embedded in epoxy resin. The cells were then thin-sectioned with a diamond knife. Sections in the range of gray to silver were collected on 150-mesh grids, stained with uranyl acetate and lead citrate, and examined under a JEOL-1200 EXII electron microscope (Jeol, Tokyo, http://www.jeol.com).

Flow Cytometric Analysis

Fluorescence cell staining was performed as described previously [10]. The cells were stained with a combination of the following mouse mAbs, which were either unconjugated or conjugated to fluorescein isothiocyanate (FITC), phycoerythrin (PE), or PC5: anti-CD14, anti-CD34, anti-CD40, anti-CD45, anti-CD80, anti-CD105, anti-CD106, anti-CD117/c-kit (Beckman Coulter, Fullerton, CA, http://www.beckmancoulter.com), anti-CD34, anti-CD133 (Miltenyi Biotec), anti-CD54, anti-CD86 (Ancell, Bayport, MN, http://www.ancell.com), anti-CD31, anti-VEGFR1, anti-VEGFR2, anti-human leukocyte antigen (HLA)-DR (Sigma-Aldrich), anti-CD144, anti-CD146/H1P12, or anti-type I collagen (Chemicon, Temecula, CA, http://www.chemicon.com). When unconjugated mAbs were used, goat anti-mouse IgG $F(ab')_2$ conjugated to FITC or PE (Beckman Coulter) was used as a secondary antibody. For intracellular type I collagen staining, the cells were permeabilized and fixed using the IntraPrep permeabilization reagent (Beckman Coulter). Negative controls were cells incubated with an isotype-matched mouse mAb to an irrelevant antigen. The cells were analyzed on a FACSCalibur flow cytometer (BD Biosciences, San Diego, http://www.bdbiosciences.com) using CellQuest software.

Immunohistochemistry on Cultured Cells

The diaminobenzidine (DAB) staining of cultured cells was performed as described [10]. The primary antibodies used were rabbit polyclonal anti-Tie-2 antibody (Santa Cruz Biotechnology Inc., Santa Cruz, CA, http://www.scbt.com) or one of the following mouse mAbs: anti-CD45, anti-vimentin (Dako, Carpinteria, CA, http://www.dako.com), anti-CD34 (Ancell),

anti-CD105 (Beckman Coulter), anti-type I collagen, anti-CD144, anti-CD146, anti-human nuclei (Chemicon), anti-VEGFR1, anti-VEGFR2 (Sigma-Aldrich), anti-von Willebrand factor (anti-vWF), and anti-endothelial nitric-oxide synthase (anti-eNOS) (BD Biosciences). Negative controls were cells incubated with normal rabbit IgG or isotype-matched mouse mAb to an irrelevant antigen, instead of the primary antibody. Biotin-labeled anti-mouse or rabbit IgG antibodies combined with a streptavidin-horseradish peroxidase complex (Nichirei, Tokyo, http://www.nichirei.co.jp/english) were used for DAB staining. Nuclei were counterstained with hematoxylin. To enumerate the proportion of cells staining positive for a given marker, at least 300 cells per culture were evaluated.

Uptake of AcLDL

Cultured adherent cells were labeled with 1,1′-dioctadecyl-3,3,3′,3′-tetramethylindocarbocyanine-labeled AcLDL (Dil-AcLDL) (2.5 μg/ml) (Molecular Probes Inc., Eugene, OR, http://probes.invitrogen.com) for 1 hour at 37°C, and AcLDL uptake was evaluated by flow cytometry and by fluorescence microscopy (IX71; Olympus, Tokyo, http://www.olympus-global.com).

Analysis of mRNA Expression

The expression of mRNA was examined using reverse transcription (RT) combined with polymerase chain reaction (PCR) as described [10]. Total RNA was extracted from HUVECs, monocyte-derived ELCs, and mouse colon carcinoma cell line CT-26, and human MOMCs that had or had not been induced to differentiate for 3, 5, 7, or 14 days, using the RNeasy kit (Qiagen, Valencia, CA). First-strand cDNA synthesized from the total RNA was subjected to PCR amplification using a panel of specific primers (supplemental online Table 1) [6, 10]. The PCR products were resolved by electrophoresis on 2% agarose gels and visualized by ethidium bromide staining.

Cell Proliferation Study

Proliferating MOMCs were detected by bromodeoxyuridine (BrdU) incorporation as described previously [12]. Briefly, MOMCs were cultured in the presence of 10 μM BrdU (Sigma-Aldrich) for 2 hours before staining. After cell fixation and DNA denaturation, the cells were incubated with a rat anti-BrdU mAb (Abcam, Cambridge, U.K., http://www.abcam.com) and a mouse mAb to human nuclei or eNOS followed by incubation with AlexaFluor 488 mouse-specific IgG and AlexaFluor 568 rat-specific IgG (Molecular Probes). Cells were observed under a confocal laser fluorescence microscope (LSM5 PASCAL; Carl Zeiss, Göttingen, Germany, http://www.zeiss.com). To enumerate the proliferating human MOMCs, the number of BrdU-positive nuclei in the total number of nuclei was calculated. Apoptotic cells were also detected by incubating unfixed cells with propidium iodide (Sigma-Aldrich).

Histamine-Mediated Release of vWF

MOMCs after endothelial differentiation treatment and HUVECs were incubated with 10 μM histamine (Sigma-Aldrich) in FBS-free low-glucose DMEM for 25 minutes. Untreated and treated cells were fixed with 10% formalin and stained with a mouse anti-vWF mAb (BD Biosciences) followed by incubation with AlexaFluor 568 mouse-specific IgG (Molecular Probes) and then with FITC-conjugated mouse anti-human nuclear mAb (Chemicon).

Changes in Gene Expression Profiles in Response to Hypoxia

MOMCs after endothelial differentiation treatment and HPAECs were incubated at 37°C in 21% or 1% oxygen for 24 hours [13]. The cells were then harvested and subjected to mRNA expression analyses using RT-PCR and the TaqMan quantitative PCR system (Applied BioSystems, Foster City, CA, http://www.appliedbiosystems.com). A combination of primers and a probe specific for VEGFR1 were designed as follows: forward primer, 5′-AACACAAGATGGCAAATCAGGAT-3′; reverse primer, 5′-GGCGCCACCGCTTAAGA-3′; and probe, 5′-(FAM)-AGGTGAAAAGATCAAGAAACGTGTGAAAAC-TCC-(TAMRA)-3′, whereas those for VEGF, glyceraldehyde-3-phosphate dehydrogenase (GAPDH), and β-actin were purchased from Applied BioSystems. Expression levels were calculated from a standard curve generated by plotting the amount of PCR product against the serial amount of input normoxic HPAEC cDNA and were expressed relative to the level of the same gene under normally oxygenated conditions.

In Vitro Vascular Tube Formation

The formation of endothelial tubular structures was studied in vitro in Matrigel cultures. Briefly, MOMCs, MOMC-derived ELCs, monocyte-derived ELCs, or cultured dermal fibroblasts (10^4 or 10^5) in EBM-2 were seeded onto 24-well plates coated with Matrigel (BD Biosciences) with or without a suboptimal number of HUVECs (10^3), which was insufficient to form typical tube structures. HUVECs (10^4) cultured with HUVECs (10^3) were used as a positive control. The cells were cultured at 37°C for 24 hours and observed with an IX71 inverted microscope. The total tube length was calculated from 10 randomly selected low-power fields for each experiment. In some experiments, MOMCs (10^4) were labeled with the green fluorescent cell linker PKH67 (Sigma-Aldrich) or Dil-AcLDL before being added to the Matrigel culture with unlabeled HUVECs (10^3). Dil-AcLDL-labeled MOMCs cultured in Matrigel for 1 or 3 days were collected using a Cell Recovery Solution (BD Biosciences), cytospun, and stained with mouse anti-eNOS or anti-CD45 mAb, followed by incubation with AlexaFluor 488 mouse-specific IgG and DAPI.

Mouse Model for In Vivo Tumor Neovascularization

All procedures were performed on severe combined immunodeficient (SCID) mice obtained from Charles River Japan (Yokohama, Japan, http://www.crj.co.jp), which were kept in specific pathogen-free conditions according to the Keio University Animal Care and Use Committee guidelines. Syngeneic murine colon carcinoma CT-26 cells (2.5×10^5) were transplanted subcutaneously into the back of SCID mice, with or without MOMCs, MOMC-derived ELCs (10^4 or 10^5), monocyte-derived ELCs, monocytes, or macrophages (10^5). Subcutaneous tumor sizes were measured by external caliper, and tumor volume was calculated with the following formula: volume = 0.5 × longest diameter × (shortest diameter)^2. Subcutaneous tumors were removed 10 days after the transplantation, and then formalin-fixed, paraffin-embedded specimens were

sectioned and stained with hematoxylin and eosin. The number of erythrocyte-bearing blood vessels was counted in 10 independent fields, and the results were expressed as the number per 1 mm^3. Frozen sections (10-μm thick) of the tumor were subjected to immunohistochemistry, in which the slides were incubated with a rat mAb to mouse-specific CD31 (BD Biosciences) or a rabbit polyclonal antibody to human-specific CD31 (Santa Cruz Biotechnology) in combination with a mouse mAb to human-specific CD31, HLA class I (Sigma-Aldrich), or vWF (BD Biosciences), followed by incubation with AlexaFluor 488 mouse-specific IgG and AlexaFluor 568 rat- or rabbit-specific IgG (Molecular Probes). Nuclei were counterstained with TO-PRO3 (Molecular Probes). These slides were examined with a confocal laser fluorescence microscope. The proportion of blood vessels containing human CD31-expressing endothelial cells in at least 100 blood vessel sections was calculated. Moreover, we calculated the proportion of cells expressing human CD31 in at least 100 HLA class I-positive cells.

Statistical Analysis

All continuous variables were expressed as the mean ± SD. Comparisons between two groups were tested for statistical significance using the Mann-Whitney test.

Results

Endothelial Differentiation of MOMCs

Human MOMCs took on a spindle shape in culture (Fig. 1A) and consisted of a single phenotypic population positive for CD14, CD45, CD34, and type I collagen by flow cytometric analysis (>96% homogeneous), as reported previously [10]. To investigate whether MOMCs could differentiate along the endothelial lineage, the MOMCs were replated on new fibronectin-coated plates and subjected to endothelial induction culture with EBM-2. During 7 days of culture, the morphology of the MOMCs changed from spindle-shaped to caudate or round with eccentric nuclei and extended cytoplasm (Fig. 1B). The proportion of spindle-shaped cells decreased with time, and nearly all the adherent cells had the caudate morphology on day 7. Electron microscopic analysis of MOMCs cultured under the endothelial induction conditions for 7 days revealed many cytoplasmic granules containing an electron-dense material. These rod-shaped microtubulated structures resembled Weibel-Palade bodies [14] and were detected in all the cells subjected to the endothelial induction treatment (Fig. 1C).

MOMCs cultured in EBM-2 for 7 days were then examined by immunohistochemistry for the expression of endothelial markers. As shown in Figure 1D, MOMC-derived ELCs expressed CD34, CD144, CD105, VEGFR1, VEGFR2, vWF, eNOS, CD146, and Tie-2, typical of endothelial cells. This set of endothelial markers was detected in nearly all the adherent cells, but the intensity of staining for vWF, eNOS, and CD146 was variable. The mRNA expression over time of selected endothelial markers and hematopoietic/monocytic markers in MOMCs undergoing endothelial induction treatment was further examined by RT-PCR (Fig. 1E). The mRNA expression of VEGFR1, VEGFR2, CD144, Tie-2, and vWF was upregulated during the first 7 days of culture and then plateaued, but the expression of VEGFR2 was downregulated on day 14. The expression of CD45 and CD14 was markedly downregulated

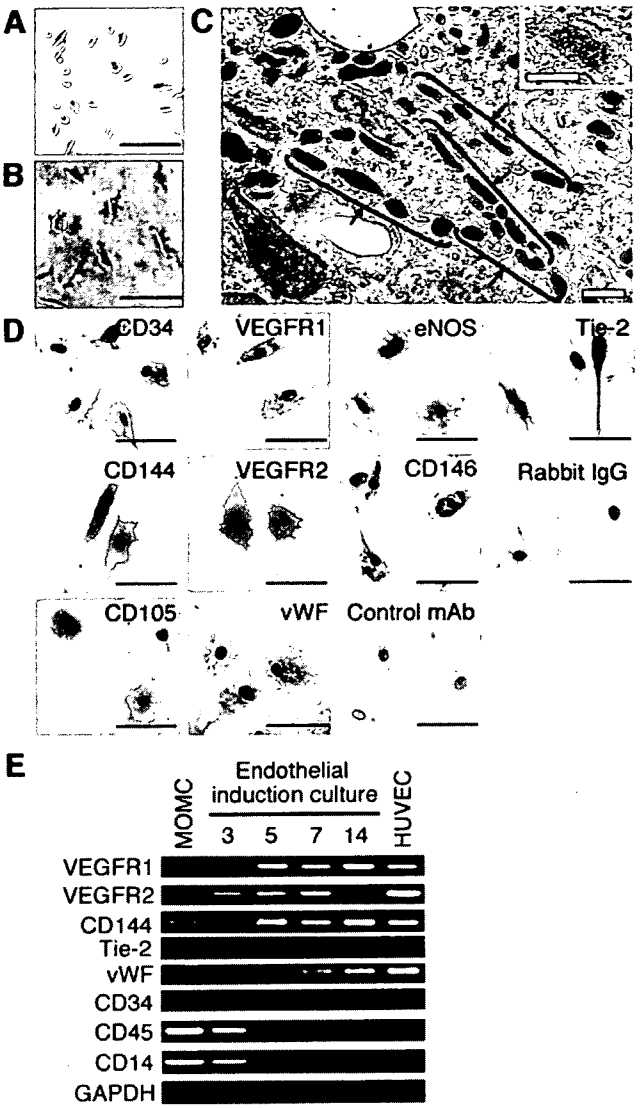

Figure 1. Morphology and protein and mRNA expression profiles of MOMC-derived endothelial-like cells. **(A, B):** Phase-contrast images of MOMCs before **(A)** and after **(B)** endothelial induction for 7 days. Scale bars = 100 μm. **(C):** A transmission electron microscopic image of MOMC-derived endothelial-like cells. Scale bar = 1 μm. Many cytoplasmic granules containing electron-dense material were observed (arrows). Inset shows an electron-dense rod-shaped inclusion at higher magnification; scale bar = 0.5 μm. Results shown are representative of 50 cells prepared in three independent experiments. **(D):** Immunohistochemical analysis of MOMCs undergoing endothelial induction for 7 days. Cells were stained with a mouse mAb or polyclonal antibody to the endothelial marker, as indicated. Controls were incubated with an isotype-matched mouse mAb to an irrelevant antigen (control mAb) or normal rabbit IgG (rabbit IgG). Nuclei were counterstained with hematoxylin. Scale bars = 50 μm. Results shown are representative of at least five independent experiments. **(E):** Reverse transcription-polymerase chain reaction analysis for mRNA expression of VEGFR1, VEGFR2, CD144, Tie-2, vWF, CD34, CD45, CD14, and GAPDH in untreated MOMCs; MOMCs with endothelial induction for 3, 5, 7, and 14 days; and HUVECs. Abbreviations: eNOS, endothelial nitric-oxide synthase; GAPDH, glyceraldehyde-3-phosphate dehydrogenase; HUVEC, human umbilical vein endothelial cell; mAb, monoclonal antibody; MOMC, monocyte-derived multipotential cell; VEGFR, vascular endothelial growth factor receptor; vWF, von Willebrand factor.

Table 1. Protein expression profiles of MOMC-derived ELCs, various monocyte-derived cells, and HUVECs

	Circulating monocytes	MOMCs	MOMC-derived ELCs	Monocyte-derived ELCs	Macrophages	HUVECs
CD45[a,b]	++	++	+	++	++	−
CD14[a]	++	++	±	+	++	−
HLA-DR[a]	++	++	+	+	++	−
CD40[a]	+	+	+	+	++	+
CD80[a]	−	−	−	−	++	−
CD86[a]	+	+	+	+	++	−
CD54[a]	+	+	+	+	+	+
CD106[a]	−	−	+	±	−	−
CD34[a,b]	−	+	+	+	−	++
CD105/endoglin[a,b]	−	+	+	+	−	++
CD117/c-kit[a]	−	−	−	−	−	−
CD133[a]	−	−	−	−	−	−
CD31[a]	+	+	+	+	+	++
CD144/VE-cadherin[a,b]	−	+	+	+	−	+
CD146[a,b]	−	−	+	−	−	++
Flt-1/VEGFR1[a,b]	−	+	+	+	−	+
Flk-1/VEGFR2[a,b]	−	−	+	−	−	+
vWF[b]	−	−	+	±	−	++
eNOS[b]	−	−	+	+	−	++
Tie-2[b]	−	+	++	+	−	+
Type I collagen[b]	−	+	+	−	−	−
AcLDL[a,b]	+	++	++	++	++	++

Consistent results were obtained in at least five independent experiments. −, no staining; ±, weak staining, +, moderate staining; ++, strong staining.

[a]Assessed by flow cytometry.

[b]Assessed by immunohistochemistry.

Abbreviations: AcLDL, acetylated low-density lipoprotein; ELC, endothelial-like cell; eNOS, endothelial nitric-oxide synthase; HLA-DR, human leukocyte antigen-DR; HUVEC, human umbilical vein endothelial cell; MOMC, monocyte-derived multipotential cell; VE, vascular endothelial; VEGFR, vascular endothelial growth factor receptor; vWF, von Willebrand factor.

during the differentiation process, whereas CD34 expression remained constant up to day 14. Notably, the mRNA expression profile of MOMCs subjected to the endothelial induction culture for 7 days was indistinguishable from the profile of HUVECs.

These results together indicate that MOMCs can differentiate into ELCs that have morphologic and phenotypic characteristics similar to those of mature endothelial cells. This endothelial differentiation was consistently observed for MOMCs derived from 20 different healthy adult donors. In addition, a similar yield of ELCs was obtained when the same culture conditions were used for the $CD14^+$ cell-enriched MOMC fraction (>99% homogeneous), MOMCs generated from freshly isolated $CD14^+$ monocytes in $CD14^-$ cell-conditioned medium, or MOMCs generated from $CD34^+$ cell-depleted PBMCs.

Phenotypes of ELCs Derived from MOMCs and Freshly Isolated Monocytes

Several reports show that ELCs can also be generated from freshly isolated circulating $CD14^+$ monocytes by culturing them with a combination of angiogenic growth factors [5–9]. The protein expression profiles of MOMC-derived ELCs on day 7 were examined by flow cytometry and/or immunohistochemistry and compared with those of ELCs prepared by culturing freshly isolated circulating monocytes in EBM-2 for 7 days (Table 1). Representative flow cytometric analyses of the cell-surface expression of CD45, CD14, CD34, CD144, and CD146 are shown in Figure 2. Monocyte-derived ELCs displayed weak CD34 and CD144 expression and downregulated CD45 expression, as described previously [6, 7]. Comparison of the expression profiles obtained from ELCs derived from different sources showed that the MOMC-derived ELCs had a higher expression of CD34, CD144, and CD146 and a lower expression of CD45 and CD14 than the monocyte-derived ELCs. Moreover, no protein expression of VEGFR2 and vWF was apparent in the monocyte-derived ELCs under our culture and immunohistochemical conditions (Table 1).

Proliferative Capacity of MOMCs During Endothelial Differentiation

To evaluate whether MOMCs proliferate during endothelial differentiation, the number of adherent cells in the MOMC cultures with and without the endothelial induction treatment were evaluated over time (Fig. 3A). The number of MOMCs increased during culture. However, MOMC expansion in endothelial induction medium (EBM-2) was sustained up to day 7, whereas the cell expansion slowed after day 3 in cultures with regular medium (low-glucose DMEM plus 10% FBS), resulting in a statistical difference in the cell number after day 5. To confirm the difference in cell division, the proportion of dividing cells in MOMC cultures over time was evaluated by BrdU incorporation. Representative immunofluorescence images of MOMCs cultured in EBM-2 and DMEM on days 1 and 5 are shown in Figure 3B. More than 25% of the MOMCs undergoing the endothelial induction treatment incorporated BrdU on days 1 and 5, but only a small propor-

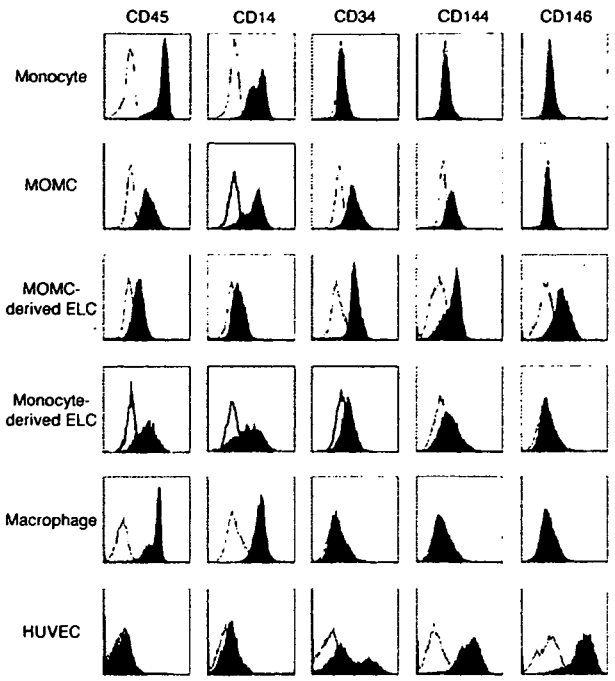

Figure 2. Flow cytometric analysis of freshly isolated circulating monocytes, undifferentiated MOMCs, MOMC-derived ELCs, monocyte-derived ELCs, macrophages, and HUVECs. MOMCs and monocytes after endothelial induction for 7 days were used as MOMC- and monocyte-derived ELCs, respectively. Cells were stained with monoclonal antibodies (mAbs) as indicated and analyzed by flow cytometry. Expression of the molecules of interest is shown as shaded histograms. Open histograms represent staining with isotype-matched control mAb. Results shown are representative of at least three independent experiments. Abbreviations: ELC, endothelial-like cell; HUVEC, human umbilical vein endothelial cell; MOMC, monocyte-derived multipotential cell.

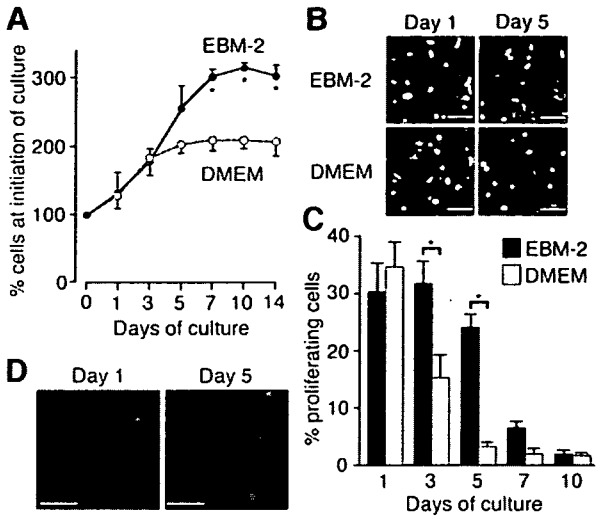

Figure 3. Proliferative capacity of MOMCs during endothelial differentiation. **(A):** The number of adherent cells in cultures of MOMCs with endothelial induction treatment (EBM-2) or without the treatment (low-glucose DMEM plus 10% fetal bovine serum [FBS]) for up to 14 days. The number of attaching cells per 1 mm^3 was counted in 10 randomly selected fields and expressed relative to the number of cells before endothelial induction. Results shown are the mean and SD from five independent donors. Asterisk indicates a statistically significant difference between the two cultures. **(B):** MOMCs were cultured for 1 or 5 days in EBM-2 or low-glucose DMEM plus 10% FBS, and bromodeoxyuridine (BrdU) incorporation during a 2-hour incubation was examined by immunohistochemistry with monoclonal antibodies (mAbs) to human nuclei (green) and BrdU (red). Yellow indicates a proliferating cell positive for both human nuclei and BrdU. Scale bars = 50 μm. **(C):** Proportion of proliferating MOMCs in culture with EBM-2 or low-glucose DMEM plus 10% FBS over time. The number of BrdU-positive nuclei divided by the total number of nuclei was calculated as the proportion of proliferating MOMCs. At least 200 cells were counted for each BrdU staining. Results are expressed as the mean and SD of four independent experiments. Asterisk indicates a statistically significant difference between the two cultures. **(D):** MOMCs were cultured for 1 or 5 days in EBM-2 and subjected to immunohistochemistry with mAbs to endothelial nitric-oxide synthase (green) and BrdU (red). Scale bars = 50 μm. Abbreviations: DMEM, Dulbecco's modified Eagle's medium; EBM-2, endothelial cell basal medium-2.

tion of the MOMCs cultured in regular medium were proliferating on day 5. Semiquantitative assessment of the $BrdU^+$ proliferating cells showed that the MOMC proliferation was greater in the endothelial induction culture than in the regular culture on days 3 and 5 (Fig. 3C). The proportion of apoptotic adherent cells positive for propidium iodide staining was <3% at all time points. When MOMCs cultured in EBM-2 were examined for BrdU incorporation and eNOS expression, nearly all cells expressing eNOS failed to incorporate BrdU at day 5 (Fig. 3D), indicating that proliferating cells are predominantly undifferentiated MOMCs.

Functional Characteristics of MOMC-Derived ELCs

We next performed a series of analyses to test whether the MOMC-derived ELCs had the functional properties of endothelial cells. First, we evaluated the capacity in vitro of MOMC-derived ELCs to release vWF in response to stimulation with histamine, which is one of the unique features of endothelial cells [15]. HUVECs and MOMC-derived ELCs were incubated with or without histamine and stained with anti-vWF and anti-nuclear mAbs (Fig. 4A). Almost half of the untreated HUVECs showed vWF throughout the cytoplasm, which disappeared after histamine treatment. Similarly, the histamine treatment resulted in a loss of vWF staining in the MOMC-derived ELCs. Another characteristic of endothelial cells is that they take up AcLDL [16]. MOMC-derived ELCs rapidly incorporated Dil-AcLDL similarly to HUVECs; however, undifferentiated MOMCs and even freshly isolated monocytes were also able to take up Dil-AcLDL (Table 1).

Endothelial cells are known to respond to hypoxia by up-regulating several molecules associated with angiogenesis and glucose regulation, such as VEGF, VEGFR1 [13], and GAPDH [17]. HPAECs and MOMC-derived ELCs were exposed to a hypoxic or normoxic condition for 24 hours, and the mRNA expression levels of VEGF, VEGFR1, GAPDH, and β-actin were compared between these two cultures. The results obtained from HPAECs and MOMC-derived ELCs were concordant and showed an increased expression of VEGF, VEGFR1, and GAPDH upon exposure to the hypoxic condition (Fig. 4B).

In Vitro Angiogenic Properties of MOMCs

We next tested whether undifferentiated MOMCs or MOMC-derived ELCs could form tubular structures when plated on Matrigel. We also tested monocyte-derived ELCs, freshly iso-

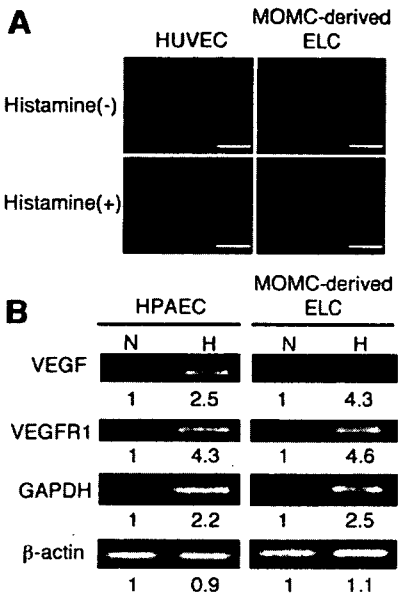

Figure 4. Functional characterization of MOMC-derived ELCs. **(A):** Histamine-mediated release of von Willebrand factor (vWF) from HUVECs and MOMC-derived ELCs. Cells were treated with or without histamine for 25 minutes and subjected to immunohistochemistry with monoclonal antibodies to vWF (red) and human nuclei (green). Representative examples of five experiments from three donors are shown. Scale bars = 50 μm. **(B):** Upregulation of mRNA for VEGF and VEGFR1 in MOMC-derived ELCs by hypoxic exposure. Cultured HPAECs and MOMC-derived ELCs were incubated in 20% O_2 (N) and 1% O_2 (H) for 24 hours, and the VEGF, VEGFR1, GAPDH, and β-actin mRNA expression was detected by reverse transcription-polymerase chain reaction (PCR). Expression levels were determined by TaqMan quantitative PCR and divided by the level of each gene under normally oxygenated conditions. Results shown are representative of three independent experiments, and the relative expression was the mean of three experiments. Abbreviations: ELC, endothelial-like cell; GAPDH, glyceraldehyde-3-phosphate dehydrogenase; H, hypoxia; HPAEC, human pulmonary artery endothelial cell; HUVEC, human umbilical vein endothelial cell; MOMC, monocyte-derived multipotential cell; N, normoxia; VEGF, vascular endothelial growth factor; VEGFR, vascular endothelial growth factor receptor.

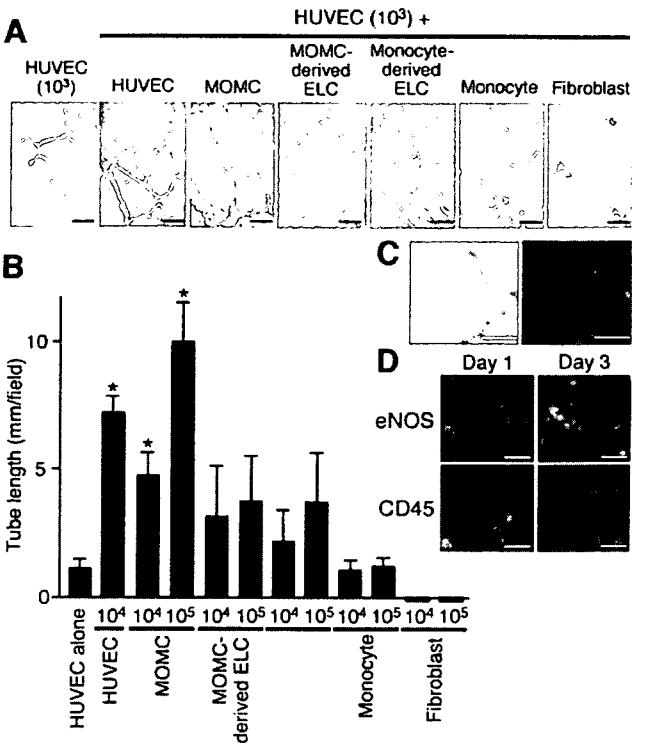

Figure 5. In vitro tubule formation promoted by various monocyte-originated cells in Matrigel culture. **(A):** HUVECs (10^3) were cultured alone or in combination with HUVECs, MOMCs, MOMC-derived ELCs, monocyte-derived ELCs, freshly isolated circulating monocytes, or cultured dermal fibroblasts (10^4) on Matrigel for 24 hours. Representative pictures of five independent experiments are shown. Scale bars = 500 μm. **(B):** Total tube length in the Matrigel cultures of HUVECs (10^3) alone and HUVECs (10^3) plus HUVECs (10^4), MOMCs, MOMC-derived ELCs, monocyte-derived ELCs, freshly isolated circulating monocytes, or cultured dermal fibroblasts (10^4 or 10^5). The combined length of the tubes was calculated from 10 randomly selected low-power fields in individual experiments, and results are expressed as the mean and SD from five independent experiments. Asterisk indicates a significantly different from HUVECs (10^3) alone. **(C):** MOMCs were previously labeled with PKH2 (10^4) and cultured on Matrigel with unlabeled HUVECs (10^3) for 24 hours. Light microscopic (top) and fluorescent (bottom) images of the same sample are shown. Scale bars = 500 μm. Results shown are representative of four independent experiments. **(D):** MOMCs were previously labeled with 1,1′-dioctadecyl-3,3,3′,3′-tetramethylindocarbocyanine-labeled acetylated low-density lipoprotein (10^4) and cultured on Matrigel with unlabeled HUVECs (10^3) for 1 or 3 days. The cells were recovered, cytospun, and examined by immunohistochemistry with monoclonal antibodies to eNOS or CD45 (green). Scale bars = 50 μm. Results shown are representative of three independent experiments. Abbreviations: ELC, endothelial-like cell; eNOS, endothelial nitric oxide synthase; HUVEC, human umbilical vein endothelial cell; MOMC, monocyte-derived multipotential cell.

lated monocytes, and cultured dermal fibroblasts. None of the monocyte-originating cells formed typical tubular structures by themselves. Therefore, a suboptimal number of HUVECs (10^3), which induce the formation of a small number of short tubular structures when cultured alone, were cocultured with the series of monocyte-derived cells and fibroblasts (10^4) (Fig. 5A). Undifferentiated MOMCs dramatically promoted the formation of tubules in the Matrigel culture with HUVECs, but only some tubules were extended in cultures of ELCs derived from MOMCs and monocytes. Freshly isolated monocytes or fibroblasts failed to enhance the formation of tubules. Compared with the culture of HUVECs (10^3) alone, semiquantitative analysis of the tube length revealed a statistically significant enhancement in the culture of undifferentiated MOMCs with HUVECs and in the positive control culture of HUVECs (10^4) (Fig. 5B). To test whether MOMCs were integrated into the tubular structures, the cells were labeled with PKH67 before the Matrigel culture with unlabeled HUVECs. PKH67-labeled MOMCs were clearly incorporated into the tubular structure (Fig. 5C). When DiI-AcLDL-labeled MOMCs were cultured with HUVECs in Matrigel, endothelial differentiation of MOMCs was accelerated based on upregulated eNOS expression and downregulated CD45 expression at day 3 (Fig. 5D).

In Vivo Vasculogenic Properties of MOMCs

To further examine the in vivo vasculogenic properties of various monocyte-derived cells, murine colon carcinoma CT-26 cells were transplanted into the back of SCID mice, alone or with human MOMCs, MOMC-derived ELCs, monocyte-de-

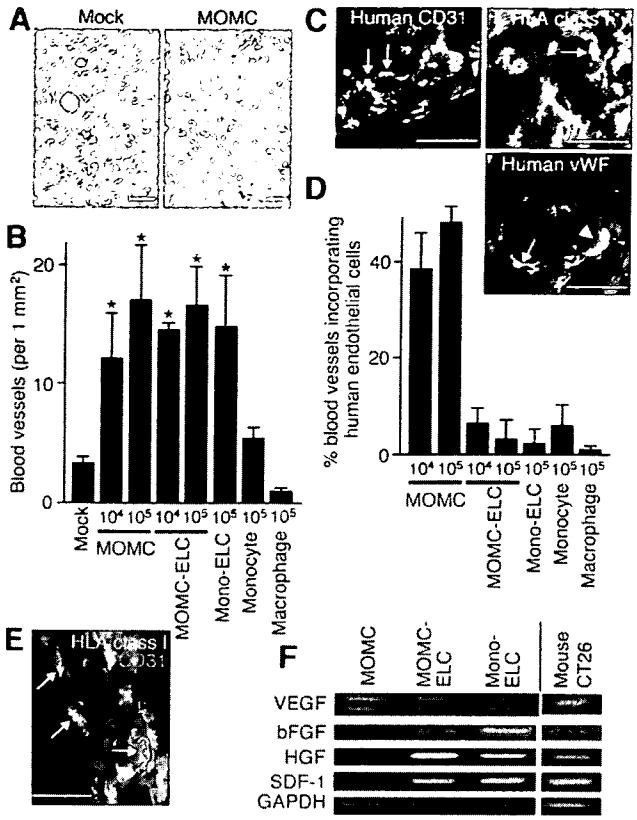

Figure 6. In vivo tumor vasculogenesis promoted by various human monocyte-derived cells in severe combined immunodeficient (SCID) mice. Murine colon carcinoma cells (CT26) were transplanted into the back of SCID mice, alone or with human MOMCs, MOMC-derived ELCs, monocyte-derived ELCs, monocytes, or macrophages, and tumor tissue sections were obtained 10 days later. **(A):** Representative tumor sections stained with hematoxylin and eosin obtained from mice receiving transplants of CT26 alone (mock) or CT26 and human MOMCs. Circles indicate blood vessels carrying erythrocytes. Scale bars = 100 μm. **(B):** Blood vessel density in tumors from mice receiving transplants of CT26 alone (mock), CT26 in combination of MOMCs, MOMC-derived ELCs (10^4 and 10^5), monocyte-derived ELCs, monocytes, and macrophages (10^5). The number of blood vessels per 1 mm^3 was calculated from 10 randomly selected fields per individual experiment, and results are expressed as the mean and SD of five independent experiments. Asterisk indicates a significant difference from mock. **(C):** Representative tumor sections from mice receiving transplants of CT26 and MOMCs, which were stained for mouse CD31 (red) and human CD31, HLA class I, or human vWF (green). Nuclei were counterstained with TO-PRO3. Arrow denotes human MOMCs that are incorporated into vascular structure and differentiated into endothelial cells, whereas arrowhead denotes human MOMCs expressing endothelial markers existing outside of the vascular lumen. Scale bars = 50 μm (human CD31) and 25 μm (HLA class I and human vWF). The results shown are representative of five experiments. **(D):** The proportion of blood vessel sections incorporating human endothelial cells in tumors from mice receiving transplants of CT26 with MOMCs, MOMC-derived ELCs (10^4 and 10^5), monocyte-derived ELCs, monocytes, and macrophages (10^5). At least 100 blood vessel sections were observed, and the proportion of vessels containing human CD31-positive endothelial cells was calculated. Results are expressed as the mean and SD of five independent experiments. **(E):** Representative tumor sections from mice receiving transplants of CT26 and MOMCs, which were stained for human CD31 (red) and HLA class I (green). Nuclei were counterstained with TO-PRO3. Yellow indicates a human cell positive for CD31. Scale bar = 50 μm. **(F):** Reverse transcription-polymerase chain reaction analysis for mRNA expression of human or mouse VEGF, bFGF, HGF, SDF-1, and GAPDH in human MOMCs, human MOMC-derived ELCs, human monocyte-derived ELCs, and murine colon carcinoma cell line CT-26. Abbreviations: bFGF, basic fibroblast growth factor; ELC, endothelial-like cell; GAPDH, glyceraldehyde-3-phosphate dehydrogenase; HGF, hepatocyte growth factor; HLA, human leukocyte antigen; MOMC, monocyte-derived multipotential cell; SDF-1, stromal cell-derived factor 1; VEGF, vascular endothelial growth factor; vWF, von Willebrand factor.

rived ELCs, freshly isolated circulating monocytes, or macrophages. At day 10, tumor sizes in MOMC-transplanted mice tended to be larger than those in mice transplanted with macrophages (48.6 ± 7.4 vs. 39.7 ± 7.2), but this difference did not reach statistical significance. Hematoxylin-eosin-stained tumor sections obtained 10 days after transplantation from the MOMC-transplanted mice showed many blood vessels carrying erythrocytes. In contrast, only a few vessels were seen in the tumor sections from the mock-treated mice receiving CT-26 alone (Fig. 6A). A semiquantitative assessment of the number of tumor blood vessels revealed that the tumors in mice receiving CT-26 transplanted with MOMCs, MOMC-derived ELCs, and monocyte-derived ELCs had significantly more vessels than did tumors from mice receiving CT-26 alone, whereas monocytes or macrophages failed to promote tumor vasculogenesis (Fig. 6B).

All the tumors were then stained with human-specific CD31, HLA class I, or vWF mAb, combined with an anti-mouse CD31 mAb. Tumors obtained from the mice that received transplants of undifferentiated MOMCs had blood vessels that included cells expressing human-specific CD31, HLA class I, or vWF but did not coexpress mouse CD31 (Fig. 6C). These findings indicate that human MOMC-derived endothelial cells contributed to tumor vasculogenesis in vivo by being incorporated and differentiating into the endothelium, although human cells expressing endothelial markers were occasionally detected outside of the vascular lumen (Fig. 6C, arrowhead). To better address the degree of tumor vessel integration, the proportion of vessel sections containing human $CD31^+$ cells was evaluated semiquantitatively (Fig. 6D). In tumors from mice receiving human MOMC transplants, approximately 40% of the tumor vessels incorporated human endothelial cells. In contrast, the proportion of human endothelial cells was less than 10% in the tumors from mice receiving MOMC-derived or monocyte-derived ELCs, even though these cells significantly promoted blood vessel formation. However, efficiency of endothelial differentiation in transplanted MOMCs (proportion of human $CD31^+$ cells in HLA class I-positive cells) was only 9.4% ± 5.1% (n = 8; Fig. 6E).

To evaluate the source of angiogenic factors in our tumor vasculogenesis model, mRNA expression of angiogenic factors was examined in human MOMCs, MOMC-derived ELCs, monocyte-derived ELCs, and CT-26 by RT-PCR (Fig. 6F). All of these cells expressed VEGF, bFGF, hepatocyte growth factor (HGF), and stromal cell-derived factor 1 (SDF-1), and expression of bFGF, HGF, and SDF-1 in MOMCs was upregulated after endothelial induction.

Discussion

In this study, we demonstrated that MOMCs can differentiate into endothelium of a mature phenotype with typical morpho-

logic, phenotypic, and functional characteristics. This proliferation and specific differentiation was induced in MOMCs by a combination of angiogenic growth factors. MOMCs expressed CD34 and several endothelial markers, such as CD144 and VEGFR1, even untreated, but the endothelial induction treatment resulted in their morphological change to a typical caudate appearance with structures resembling Weibel-Palade bodies, the upregulation of mature endothelial markers, and the downregulation of hematopoietic/monocytic markers. In addition, the MOMC-derived ELCs possessed in vitro functional characteristics of endothelial cells, including the release of vWF in response to the vasoactive agent histamine, the incorporation of AcLDL, and the upregulated gene expression of VEGF, VEGFR1, and GAPDH in response to hypoxia. These features were indistinguishable from those of cultured mature endothelial cells. Finally, MOMCs responded to angiogenic stimuli and promoted in vitro tubule formation in Matrigel culture and in vivo neovascularization in the setting of tumorigenesis. The MOMC's contribution of endothelial cells to vessels in the in vivo tumor model was nearly 40%, a level similar to those of other sources of endothelial progenitors [18–20], but only 10% of transplanted MOMCs differentiated into endothelial cells in vivo. It has been shown that circulating monocytes play a crucial role in neovascularization, especially in collateral vessel growth (arteriogenesis) [21, 22], and an infusion of bone marrow-derived $CD34^-CD14^+$ monocytic cells contributes to the regeneration of functional endothelium through rapid endothelialization [23]. These reports and the present study together support the idea that $CD14^+$ monocytes are not solely phagocyte precursors but also precursors for endothelium, although this fate may not be expressed during normal development in the absence of cues.

Undifferentiated MOMCs were integrated into blood vessels and differentiated into endothelium in vitro and in vivo more efficiently than did MOMC-derived ELCs and monocyte-derived ELCs, although these cell types had a similar ability to induce in vivo tumor neovascularization. The lack of integration of monocyte-derived ELCs generated in the EPC culture into a growing network of vascular endothelium is consistent with a previous study [24]. In this regard, the efficiency of neovascularization is not solely attributable to the incorporation of progenitors into newly formed vessels but is also influenced by the release of proangiogenic factors. Indeed, MOMCs, MOMC-derived ELCs, and monocyte-derived ELCs produced multiple angiogenic growth factors, and these growth factors potentially play major roles in mobilizing putative endothelial progenitors from the bone marrow and stimulating the proliferation and differentiation of residential mature endothelial cells [25]. Several cultured mature endothelial cell lines do not integrate into newly formed vessels [26, 27], and this is probably because expression levels of cell adhesion molecules and soluble factors that regulate tubular formation capacity are heterogeneous among endothelial cells [28]. Similarly, ELCs subjected to the endothelial differentiation treatment promote new blood vessel formation mainly through the secretion of proangiogenic factors. This feature is consistent with a recent study showing that bone marrow-derived hematopoietic cells are recruited to an angiogenic region in response to VEGF and contribute to vasculogenesis not being integrated as endothelial cells but existing outside of vascular lumen [29]. In contrast, undifferentiated MOMCs, which share several phenotypic features with endothelial progenitors, may contribute to neovascularization by being incorporated and differentiating into the endothelium in addition to secretion of proangiogenic factors.

During embryogenesis, the commitment of the hemangioblast, a bipotent stem cell for hematopoietic and endothelial cells, to the endothelial lineage is characterized by the sequential expression of CD144, CD31, and CD34 [30, 31]. It is reported that postnatal endothelial progenitor cells can be selected from the bone marrow and peripheral blood based on their expression of CD34, CD133, and VEGFR2 [4, 32], and these progenitors also express CD144, CD31, and Tie-2 [33]. The differentiation of these progenitor cells into mature endothelial cells is accompanied by the upregulated expression of vWF and CD146. The differentiation of circulating monocytes into the endothelial lineage via MOMCs follows the same sequence of events. Specifically, monocytes acquire the expression of CD34, CD144, and Tie-2 during their differentiation into MOMCs and are further induced to express VEGFR2 and subsequently vWF and CD146 by the endothelial induction treatment. This observation suggests that the differentiation process leading to adoption of the endothelial lineage is partly shared by monocytes and hemangioblasts, although we did not detect CD133 expression in monocytes during this differentiation process.

It is unlikely that the endothelial differentiation we observed arose from nonhematopoietic circulating precursors for endothelial cells contaminating the MOMC population. In this regard, peripheral blood contains $CD34^+CD133^+VEGFR2^+$ circulating endothelial progenitors and $CD34^+CD133^-$ mature endothelial cells shed from the vessel wall, but their frequency is extremely low (<0.01% of PBMCs) [4, 33, 34]. Moreover, the depletion of $CD34^+$ cells from PBMCs before the generation of MOMCs did not affect the yield of ELCs. Although we could not entirely exclude the possibility that cell fusion was partly responsible for the phenotypic change of human MOMCs in the in vivo tumor vascularization model, we believe that the involvement of cell fusion in our observations is unlikely, because endothelial cells expressing both mouse and human CD31 were hardly ever detected in the tumor blood vessels.

MOMCs are derived from circulating $CD14^+CD34^-$ monocytes [10], but their detailed origin is unknown. Recently, two populations of circulating cells with the capacity to differentiate into endothelial cells were reported by two investigator groups [27, 35]. MOMCs appear to correspond to early EPCs, which show $CD14^+$ spindle-shape morphology and rapid differentiation into endothelial cells. However, MOMCs have limited proliferative capacity: this characteristic might be acquired through differentiation into MOMCs without angiogenic stimulation. On the other hand, Romagnani et al. have reported that circulating $CD14^+CD34^{low}$ cells, which are not detected by a standard flow cytometry or magnetic bead-based sorting but can be detected by the highly sensitive antibody-conjugated magnetofluorescent liposomes technique, exhibit both phenotypic and functional features of pluripotent stem cells [36], suggesting that $CD14^+CD34^{low}$ cells are the origin of MOMCs.

Emerging evidence suggests that the transplantation of various distinct cell types containing potential endothelial progenitors, obtained either by isolation or ex vivo cultivation from the bone marrow or peripheral blood, augments the neovascularization of ischemic tissue [25, 37]. In initial pilot studies, the introduction of autologous cells derived from the bone marrow

or peripheral blood induced a therapeutic improvement in the blood supply to ischemic tissue [38, 39]. Presently, a variety of cell types, including unfractionated bone marrow cells, bone marrow-derived CD133$^+$ cells, circulating CD133$^+$ cells mobilized by granulocyte colony-stimulating factor, and ELCs generated in the EPC culture, have been proposed as transplantable cells for therapeutic neovasculogenesis, but it remains unclear which cell source is the best for therapeutic cell transplantation to promote organ vascularization in terms of efficacy and safety. Cell therapy using MOMCs has some advantages over the currently proposed strategies using other cell sources, since peripheral blood, without progenitor cell mobilization treatment, is a relatively obtainable and safe source of autologous cells. Theoretically, $>10^8$ MOMCs could be prepared by leukapheresis [10], although the number of MOMCs requiring effective vascular regeneration therapy is unknown. Further studies comparing the clinical potential of various endothelial progenitors to restore long-lasting organ vascularization and function are necessary.

ACKNOWLEDGMENTS

This work was supported by a grant-in-aid for Scientific Research from the Japanese Ministry of Education, Science, Sports and Culture and by Keio University. We thank Noriyuki Seta for helpful discussions, Aya Komori and Yoko Tanaka for expert technical assistance, and Toshihiro Nagai and Yoko Ogawa for assisting in the electron microscopic analysis.

DISCLOSURES

The authors indicate no potential conflicts of interest.

REFERENCES

1 Rafii S. Circulating endothelial precursors: Mystery, reality, and promise. J Clin Invest 2000;105:17–19.

2 Hristov M, Erl W, Weber PC. Endothelial progenitor cells: Mobilization, differentiation, and homing. Arterioscler Thromb Vasc Biol 2003;23:1185–1189.

3 Asahara T, Murohara T, Sullivan A et al. Isolation of putative progenitor endothelial cells for angiogenesis. Science 1997;275:964–967.

4 Peichev M, Naiyer AJ, Pereira D et al. Expression of VEGFR-2 and AC133 by circulating human CD34$^+$ cells identifies a population of functional endothelial precursors. Blood 2000;95:952–958.

5 Harraz M, Jiao C, Hanlon HD et al. CD34$^-$ blood-derived human endothelial cell progenitors. STEM CELLS 2001;19:304–312.

6 Fernandez Pujol B, Lucibello FC, Gehling UM et al. Endothelial-like cells derived from human CD14$^+$ monocytes. Differentiation 2000;65:287–300.

7 Schmeisser A, Garlichs CD, Zhang H et al. Monocytes coexpress endothelial and macrophagocytic lineage markers and form cord-like structures in Matrigel® under angiogenic conditions. Cardiovasc Res 2001;49:671–680.

8 Rehman J, Li J, Orschell CM et al. Peripheral blood "endothelial progenitor cells" are derived from monocyte/macrophages and secrete angiogenic growth factors. Circulation 2003;107:1164–1169.

9 Urbich C, Heeschen C, Aicher A et al. Relevance of monocytic features for neovascularization capacity of circulating endothelial progenitor cells. Circulation 2003;108:2511–2516.

10 Kuwana M, Okazaki Y, Kodama H et al. Human circulating CD14$^+$ monocytes as a source of progenitors that exhibit mesenchymal cell differentiation. J Leukoc Biol 2003;74:833–845.

11 Kodama H, Inoue T, Watanabe R et al. Cardiomyogenic potential of mesenchymal progenitors derived from human circulating CD14$^+$ monocytes. Stem Cell Dev 2005;14:676–686.

12 Kodama H, Inoue T, Watanabe R et al. Neurogenic potential of progenitors derived from human circulating CD14$^+$ monocytes. Immunol Cell Biol 2006;84:209–217.

13 Gerber HP, Condorelli F, Park J et al. Differential transcriptional regulation of the two vascular endothelial growth factor receptor genes. J Biol Chem 1997;272:23659–23667.

14 Wagner DD, Olmsted JB, Marder VJ. Immunolocalization of von Willebrand protein in Weibel-Palade bodies of human endothelial cells. J Cell Biol 1982;95:355–360.

15 Rosenberg JB, Foster PA, Kaufman RJ et al. Intracellular trafficking of factor VIII to von Willebrand factor storage granules. J Clin Invest 1998;101:613–624.

16 Steinberg D, Pittman RC, Carew TE. Mechanisms involved in the uptake and degradation of low density lipoprotein by the artery wall in vivo. Ann N Y Acad Sci 1985;454:195–206.

17 Graven KK, Troxler RF, Kornfeld H et al. Regulation of endothelial cell glyceraldehydes-3-phosphate dehydrogenase expression by hypoxia. J Biol Chem 1994;269:24446–24453.

18 Conway EM, Collen D, Carmeliet P. Molecular mechanisms of blood vessel growth. Cardiovasc Res 2001;49:507–521.

19 Ribatti D, Vacca A, Nico B et al. Postnatal vasculogenesis. Mech Dev 2001;100:157–163.

20 Reyes M, Dudek A, Jahagirdar B et al. Origin of endothelial progenitors in human postnatal bone marrow. J Clin Invest 2002;109:337–346.

21 Pipp F, Heil M, Issbrucker K et al. VEGFR-1-selective VEGF homologue PlGF is arteriogenic: Evidence for a monocyte-mediated mechanism. Circ Res 2003;92:378–385.

22 Heil M, Ziegelhoeffer T, Pipp F et al. Blood monocyte concentration is critical for enhancement of collateral artery growth. Am J Physiol Heart Circ Physiol 2002;283:H2411–H2419.

23 Fujiyama S, Amano K, Uehira K et al. Bone marrow monocyte lineage cells adhere on injured endothelium in a monocyte chemoattractant protein-1-dependent manner and accelerate reendothelialization as endothelial progenitor cells. Circ Res 2003;93:980–989.

24 Rohde E, Malischnik C, Thaler D et al. Blood monocytes mimic endothelial progenitor cells. STEM CELLS 2006;24:357–367.

25 Urbich C, Dimmeler S. Endothelial progenitor cells: Characterization and role in vascular biology. Circ Res 2004;95:343–353.

26 Kocher AA, Schuster MD, Szabolcs MJ et al. Neovascularization of ischemic myocardium by human bone-marrow-derived angioblasts prevents cardiomyocyte apoptosis, reduces remodeling and improves cardiac function. Nat Med 2001;7:430–436.

27 Hur J, Yoon CH, Kim HS et al. Characterization of two types of endothelial progenitor cells and their different contributions to neovasculogenesis. Arterioscler Thromb Vasc Biol 2004;24:288–293.

28 Ikeda K, Quertermous T. Molecular isolation and characterization of a soluble isoform of activated leukocyte cell adhesion molecule that modulates endothelial cell function. J Biol Chem 2004;279:55315–55323.

29 Grunewald M, Avraham I, Dor Y et al. VEGF-induced adult neovascularization: Recruitment, retention, and role of accessory cells. Cell 2006;124:175–189.

30 Nishikawa SI, Nishikawa S, Kawamoto H et al. In vitro generation of lymphohematopoietic cells from endothelial cells purified from murine embryos. Immunity 1998;8:761–769.

31 Yamashita J, Itoh H, Hirashima M et al. Flk1-positive cells derived from embryonic stem cells serve as vascular progenitors. Nature 2000;408:92–96.

32 Gehling UM, Ergun S, Schumacher U et al. In vitro differentiation of endothelial cells from AC133-positive progenitor cells. Blood 2000;95:3106–3112.